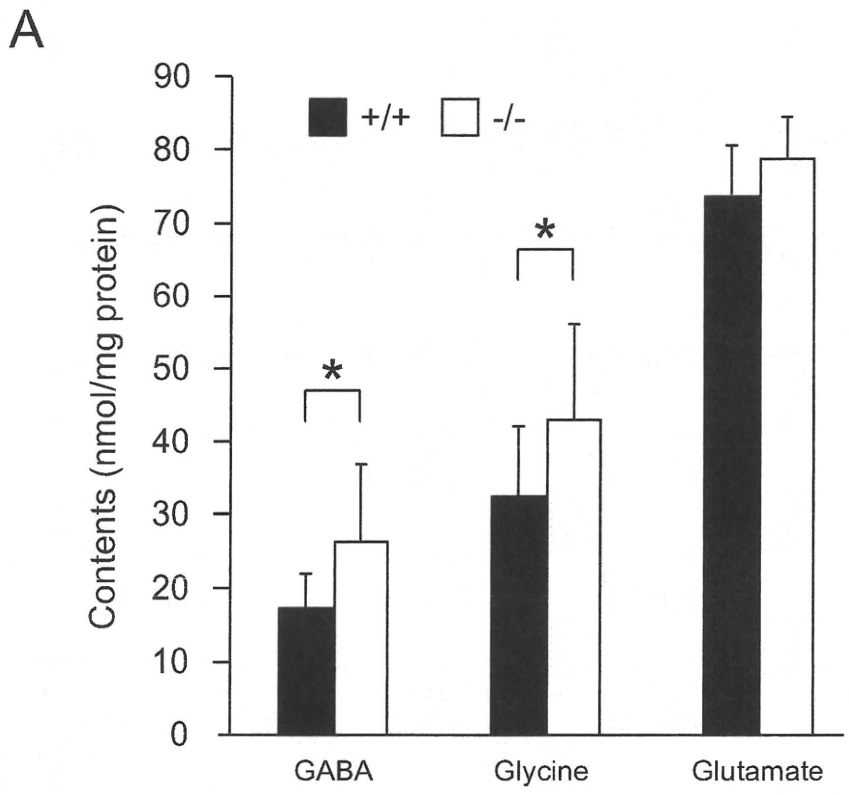

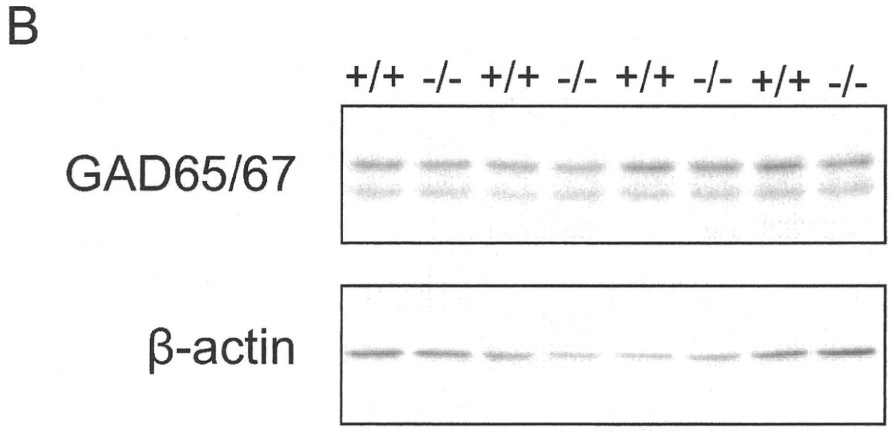

Figure 2 Neurotransmitter contents and expression levels of GAD65 and GAD67. (A) Neurotransmitter contents of E18.5 mouse forebrain. $VGAT^{-/-}$ mice showed significantly higher levels of GABA and glycine than $VGAT^{+/+}$ mice, but not glutamate. Values represent means ± SD (*P < 0.05; Student's t-test, n = 5-13 per group). (B) Western blot analysis. The expression level of GAD65 and GAD67 in whole brain homogenates was not significantly different between $VGAT^{+/+}$ (+/+) and $VGAT^{-/-}$ (-/-) mice. Equal amounts of protein were loaded and probed with an antibody that recognizes both GAD65 and GAD67. For the statistical comparison, the same blot was probed with anti-β-actin antibody as an internal control and measurements for GAD65 and GAD67 bands were normalized to the β-actin bands (GAD65: $VGAT^{+/+}$ 100 ± 23%; $VGAT^{-/-}$ 111 ± 20%, n = 4, P = 0.71) (GAD67: $VGAT^{+/+}$ 100 ± 18%; $VGAT^{-/-}$ 93 ± 17%, n = 4, P = 0.80).

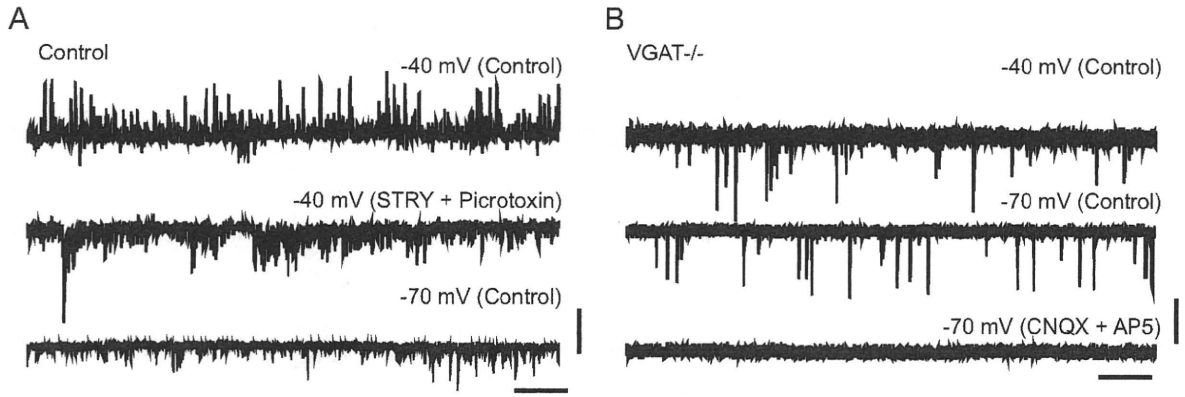

Figure 3 Electrophysiological characteristics of synaptic transmission in the VGAT$^{-/-}$ spinal cord. (A) A representative whole-cell patch-clamp recordings from control motoneurons (MNs) in a voltage clamp. In control motoneurons, spontaneous outward currents were observed when the membrane potential was held at -40 mV (upper trace). These currents were blocked by bath application of strychnine (STRY, 0.5 μM) and picrotoxin (50 μM) (middle trace). Inward currents persisted in the presence of these antagonists and became prominent when the membrane potential was held at -70 mV. (B) In VGAT$^{-/-}$ (VGAT-/-) MNs, no spontaneous outward currents were observed (upper trace). Inward currents observed at -70 mV (middle trace) were blocked by CNQX (10 μM) and AP5 (50 μM). Vertical bars indicate 100 pA (A) and 50 pA (B). Horizontal bars indicate 2 s (A, B).

GAD67 exhibit different molecular functions, we investigated whether the severity of cleft palate was different between VGAT$^{-/-}$ and GAD67$^{-/-}$ mice. Figure 5A shows hematoxylin-eosin staining of coronal sections from the oral region. In the cleft palate of VGAT$^{-/-}$ mice, the palatal shelves remained vertical along the sides of the tongue (3 of 3). However, in GAD67$^{-/-}$ mice, the palatal shelves were elevated up to a horizontal position (3 of 3). In one of the GAD67$^{-/-}$ mice, the palatal shelves even fused with each other completely (data not shown). These observations suggest that palatogenesis progresses further in GAD67$^{-/-}$ mice than in VGAT$^{-/-}$ mice. Our observations also suggest that cleft palate in VGAT$^{-/-}$ mice is more severe than in GAD67$^{-/-}$ mice.

The observation of omphalocele in VGAT$^{-/-}$ mice prompted us to investigate whether GAD67$^{-/-}$ mice displayed omphalocele. We found omphalocele in GAD67$^{-/-}$ and VGAT$^{-/-}$ mice (Figure 5B), indicating that GABA signaling is involved in its onset. The incidence rate of omphalocele in GAD67$^{-/-}$ mice was 43% (17 of 40), whereas the incidence in VGAT$^{-/-}$ mice was 100% (77 of 77; see also Table 1). Thus, the penetrance of omphalocele in GAD67$^{-/-}$ mice was lower than in VGAT$^{-/-}$ mice. The size of omphalocele appeared to be larger in VGAT$^{-/-}$ mice than in GAD67$^{-/-}$ mice. Taken together, these data suggest omphalocele in GAD67$^{-/-}$ mice is less severe than in VGAT$^{-/-}$ mice, similar to what was observed with the cleft palate.

Discussion

The present work addresses the contribution of VGAT to embryonic development. We generated VGAT mice and found that VGAT is fundamental for GABA and/or glycine release in the spinal cord. Moreover, in the absence of VGAT, there are profound effects on muscle, liver and lung during embryonic development. These observations bear important consequences for understanding the functional roles of VGAT from the cellular to the whole-body level.

Generation of VGAT knockout mice

Wojcik et al. [10] generated VGAT knockout mice, in which a mutation was inserted into exon 1, and these mice exhibit cleft palate and omphalocele. Here, we generated floxed VGAT knockout mice, in which exons 2 and 3 of the VGAT gene were flanked by loxP sites. Crossing the floxed VGAT mice to CAG-Cre mice reproduced the phenotypes of cleft palate and omphalocele. Exons 1 and 2/3 encode the cytoplasmic domain and the transmembrane domain, respectively [3,13]. Our results demonstrate that exons 2 and 3 are dispensable for the function of VGAT.

VGAT$^{floxneo/floxneo}$ mice were born at the expected frequency, were viable, did not have a cleft palate or omphalocele, and were overtly indistinguishable from their wild-type littermates. Western blot showed that the level of VGAT protein expression in VGAT$^{floxneo/floxneo}$ brain was not different from the wild-type brain (Additional file 1: Supplementary Figure S1). These results suggest that a loxP sequence and an frt-flanked phosphoglycerate kinase promoter-driven neomycin-resistance gene (PGK-Neo) inserted into intron 1 and the 3'-flanking region of the VGAT gene, respectively, do not affect the expression level of VGAT protein. Therefore, the VGAT-floxneo

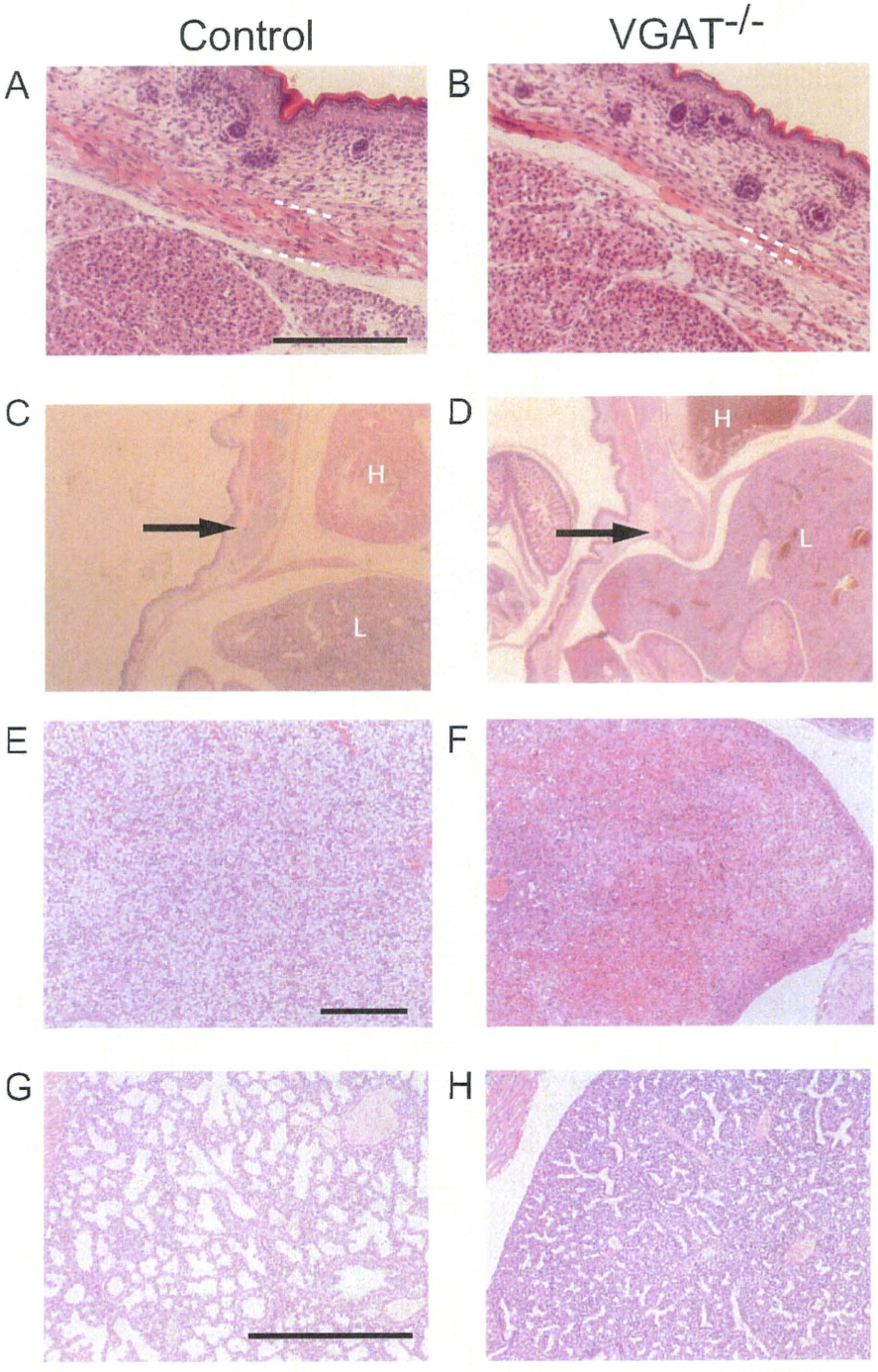

Figure 4 Histological analysis of VGAT$^{-/-}$ mice. Histological analysis (hematoxylin and eosin staining) of trapezius muscle (A, B), sagittal sections (C, D), liver (E, F) and lung (G, H) from E18.5 VGAT$^{-/-}$ mice (B, D, F, H) and control mice (A, C, E, G). (A, B) The trapezius muscle (bounded partly by white dashed lines) of VGAT$^{-/-}$ mouse (B) was thinner than the control mouse (A). Scale bar: 200 μm. (C, D) The VGAT$^{-/-}$ ribs (arrow in D) in the lower part were depressed, and their position was inside compared to the control ribs (arrow in C). H, heart; L, liver. (E, F) Red blood cell congestion was characteristic of VGAT$^{-/-}$ liver, but not control liver. Scale bar: 200 μm. (G, H) The VGAT$^{-/-}$ lung contained much less alveolar space than the control lung. Scale bar: 500 μm.

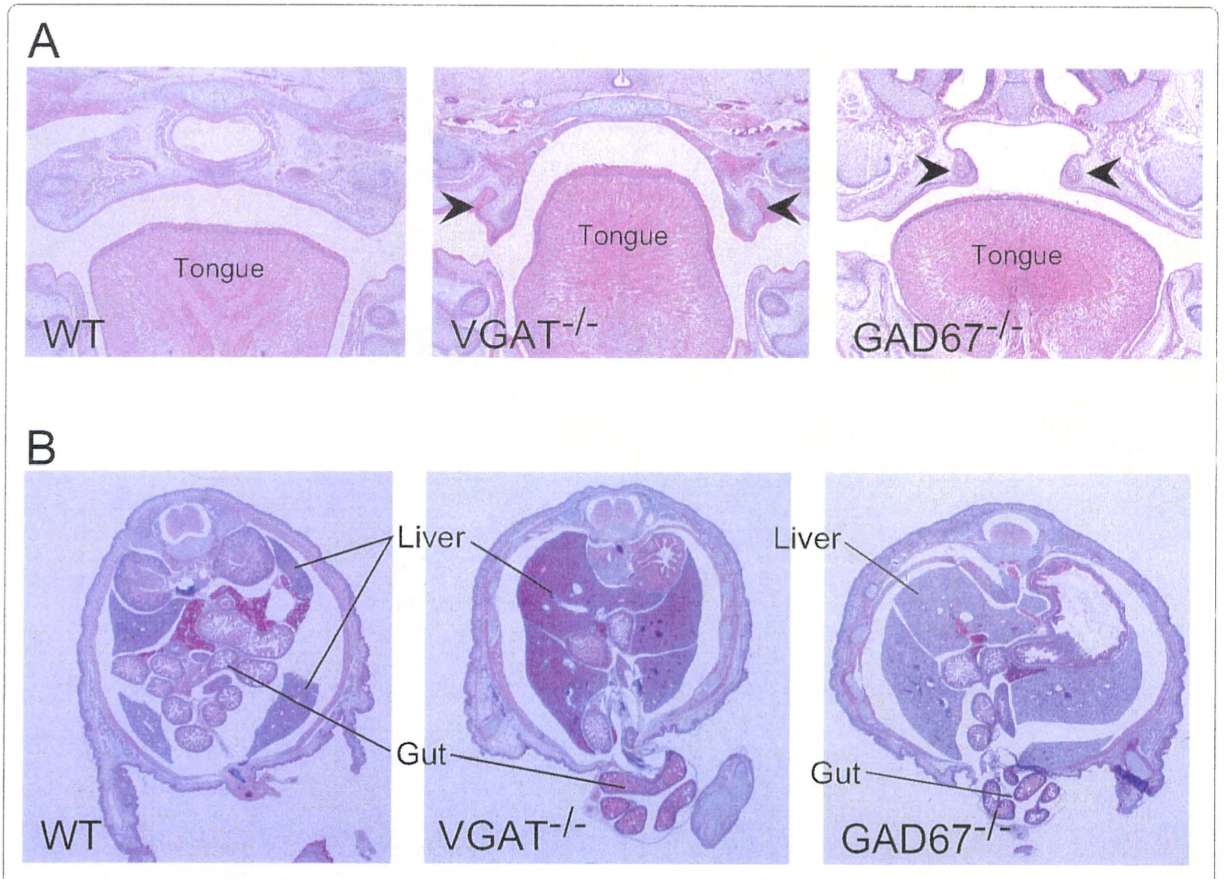

Figure 5 Histological comparison of omphalocele and cleft palate between VGAT$^{-/-}$ and GAD67$^{-/-}$ mice. (A) Hematoxylin-eosin stained coronal sections of the facial region of E18.5 wild-type (left panel), VGAT$^{-/-}$ (middle panel) and GAD67$^{-/-}$ (right panel) mice. Histological examination revealed that the secondary palatal shelves (arrowhead) of VGAT$^{-/-}$ mice were directed vertically down along the side of tongue in contrast to the fused palate of wild-type mice. In the cleft palate of GAD67$^{-/-}$ mice (right panel), palatal shelves failed to fuse but were elevated horizontally unlike those in VGAT$^{-/-}$ mice. (B) Hematoxylin-eosin stained coronal sections of the umbilical region of E18.5 wild-type (left panel), VGAT$^{-/-}$ (middle panel) and GAD67$^{-/-}$ (right panel) embryos. The ventral body wall of the VGAT$^{-/-}$ mice did not close and the gut protruded from the peritoneal cavity. In contrast to VGAT$^{-/-}$ mice, the ventral body wall of wild-type mice closed around the umbilicus, and the gut had already returned to the peritoneal cavity. The omphalocele in GAD67$^{-/-}$ mice was less severe than in VGAT$^{-/-}$ mice because a large amount of gut was observed at the umbilical level in VGAT$^{-/-}$ mice compared to GAD67$^{-/-}$ mice.

allele allowed for Cre-mediated conditional inactivation of the VGAT gene, and mice carrying these alleles will be useful in examining VGAT function at different developmental stages and in distinct cell types.

Increase of overall GABA and glycine contents in VGAT$^{-/-}$ forebrains

We showed that both GABA and glycine contents were increased in the VGAT$^{-/-}$ forebrain, but not an excitatory neurotransmitter glutamate, which is transported into synaptic vesicles by vesicular glutamate transporters. An increase in GABA content in VGAT$^{-/-}$ mice is similar to that in ACh contents in VAChT knockout mice [16], but it is opposite of the decrease in monoamine contents in vesicular monoamine transporter 2 knockout mice. In *C. elegans*, the mutational inactivation of VGAT also leads to an increase in GABA immunoreactivity in GABAergic neurons [24]. In VAChT knockout mice the amount of the ACh-synthesizing enzyme choline acetyltransferase (ChAT) is increased at the mRNA and protein levels compared to their wild-type littermates, suggesting that the change in ChAT expression may be related to a compensatory mechanism due to the lack of ACh release [16]. Conversely, the amounts of the GABA-synthesizing enzymes GAD65 and GAD67 were not different in between the brains of VGAT$^{-/-}$ mice and their control littermates (Figure 2B). Therefore, it is possible that the increased GABA in VGAT$^{-/-}$ brain was due to a reduction in their degradation. GABA and glycine are released from presynaptic

neurons into the synaptic cleft and are retrieved in neurons and glial cells by plasma membrane transporters [25,26]. GABA and glycine taken up in glial cells are further metabolized, but the GABA and glycine taken up in neurons are directly recycled into synaptic vesicles [27,28]. Because degradation systems for both GABA and glycine are mainly localized to glial cells [27,29], the transport into glial cells from the synaptic cleft is important for their degradation. Because the synaptic release of GABA and glycine was absent in $VGAT^{-/-}$ mice, the deletion of VGAT may result in little or no transport of GABA and glycine into glial cells. GABA and glycine then accumulate in the GABAergic and glycinergic neurons, respectively, but they are not degraded in the glial cells of $VGAT^{-/-}$ mice.

Contribution of VGAT to motor function

In the embryonic spinal cord of rodents, synaptic transmission to MNs mediated by GABA and glycine is prominent from the early fetal period [30,31]. Our results from the electrophysiological recordings of spinal cord MNs indicate that the inhibitory synaptic transmission was clearly absent in the VGAT knockout MNs, but that the excitatory synaptic transmission was present. Our results also suggest the absence of other functional mechanisms that transport GABA and/or glycine into synaptic vesicles in these synapses. $VGAT^{-/-}$ fetuses at E17.5-18.5 not only were completely immobile and stiff, but also none of them responded to mechanical stimuli by pinching the limb or the tail. Therefore, it is probable that the lack of inhibitory transmission onto MNs in $VGAT^{-/-}$ fetuses resulted in defects in the spontaneous and stimulus-induced movements *in vivo* despite the presence of excitatory synaptic transmission.

In addition to the defect in motor movement, trapezius muscle displayed atrophy in $VGAT^{-/-}$ mice. Embryonic myogenesis progresses by the proliferation of myoblasts and fusion of myotubes, but it requires substantial cell death [32]. Physical forces play a significant role in the development and maintenance of skeletal muscle [33]. In cultured myoblasts, chronic and cyclic stretch results in an increase in cell death, including apoptosis [34]. Therefore, a possible explanation for the atrophy in $VGAT^{-/-}$ trapezius muscle is that stretching of the trapezius muscle due to the hunched posture caused an increase in apoptosis during development.

Phenotypes of VGAT and GAD67 knockouts outside of the brain

Ventral body wall closure abnormalities, such as omphalocele, are common human birth defects, but their molecular and cellular bases are poorly understood [35]. The mouse provides a model system to study the genetic defects and environmental insults that can lead to ventral body wall closure abnormalities [20]. In this study, omphalocele was observed in $VGAT^{-/-}$ and $GAD67^{-/-}$ mice, indicating that the lack of GABA signaling was involved in its onset. Omphalocele has been observed in K^+-Cl^--cotransporter 2 (KCC2) knockout mice [36], and KCC2 is required for GABA- and/or glycine-induced hyperpolarizing responses [37]. In the KCC2 knockout mice, GABA and/or glycine signals continue to act in an excitatory, but not an inhibitory, manner. Therefore, the omphaloceles observed in both $VGAT^{-/-}$ mice and $GAD67^{-/-}$ mice resulted from defects in the inhibitory neurotransmission derived from the hyperpolarizing response. A lack of inhibitory transmission in $VGAT^{-/-}$ mice may lead to motor deficits, such as a hunched posture. It is likely that the hunched posture resulted in increases in both intrathoracic and intraabdominal pressures and this increased pressure caused omphalocele.

Concerning the mechanism of onset of cleft palate, studies using knockout mice have revealed associations between cleft palate and mutation of genes related to GABA signaling, such as *GAD67* and *GABRB3* [8,23,38]. Because the lack of the GAD67 gene leads to a reduction in tongue movement [39], the sluggish tongue may be an obstacle to development of the palatal shelves.

The cleft palate and omphalocele phenotypes were more severe in $VGAT^{-/-}$ mice than in $GAD67^{-/-}$ mice. Glycinergic transmission is present in embryonic spinal cord and brainstem [40]. Hyperekplexia is a neurogenetic disorder caused mostly by mutations in the gene encoding the α1 subunit of glycine receptor and is characterized by an exaggerated startle response and neonatal hypertonia. In patients with hyperekplexia, the recurrent abdominal muscle contraction from the exaggerated startle response can increase the abdominal pressure and lead to omphalocele and inguinal hernia [41,42]. These reports suggest that a defect in glycinergic transmission is involved in the onset of omphalocele. A small amount of GABA is synthesized by another GAD isoform, GAD65, at the embryonic stage [8,43]. The differences in the severity between $VGAT^{-/-}$ and $GAD67^{-/-}$ mice must be due to the presence of both glycinergic and GAD65-produced GABAergic transmission in $GAD67^{-/-}$ fetuses, but not in $VGAT^{-/-}$ fetuses.

Conclusion

In the present study, we established a VGAT knockout mouse, with which we demonstrated that VGAT is fundamental for GABAergic and/or glycinergic transmission. We also showed that VGAT is important for fetal growth and the development of muscle, liver and lung. The VGAT knockout mice described here may provide a useful tool for the study of specific functions of VGAT-dependent GABAergic and/or glycinergic

transmission in mice. GABAergic neurons are classified into several subtypes according to the expression of chemical markers, such as parvalbumin and somatostatin [44,45]. Therefore, our floxed VGAT mice will be useful for conditional knockout studies to further investigate the role of VGAT in GABAergic neuronal subtypes.

Methods

Animals

All animal procedures were conducted in accordance with the guiding principles of the NIH under the review and approval of the Animal Care and Experimentation Committee, Gunma University, Showa Campus (Maebashi, Japan). Every effort was made to minimize the number of animals used and their suffering.

Construction of the Targeting Vector

Genomic BAC clones containing the mouse VGAT (mVGAT) locus were purchased, and the regions covering the entire VGAT gene were subcloned [13]. A genomic fragment spanning exons 1-3 of the mVGAT gene was used for the targeting vector (Figure 1; targeting vector). The HindIII (in the 5'-flanking region) - KpnI (in the 3'-flanking region) fragment (7.5 kb) was subcloned into pBluescript II KS(-), and the 5'-loxP site was introduced into the XbaI site (in intron 1). The 5'-loxP site was flanked by a KpnI site artificially introduced for Southern blot analysis. The 7.5 kb fragment was used as the 5' homologous region containing the 5'-flanking region, exons 1-3 and the 3'-flanking region. The frt-flanked PGK-Neo cassette for positive selection of ES clones and the 3'-loxP site were inserted into the KpnI site (in the 3'-flanking region). The KpnI-BstEII fragment in the 3'-flanking region (3.5 kb) was added as the 3' homologous region. An MC1-DT-ApA cassette for negative selection [46] was ligated to the 3' end of the homologous region.

Creation of a VGAT knockout allele

The linearized targeting vector was introduced by electroporation into ES cells (CCE) of 129/SvEv mouse origin, and G418-resistant colonies were screened by Southern blot analysis using probes outside of the targeting vector. KpnI-digested genomic DNA prepared from ES cell colonies was hybridized with 5' probes. The correctly targeted ES clones were injected into C57BL/6 blastocysts to produce germline chimeras. The germline chimeras were mated with C57BL/6 mice to establish the $VGAT^{floxneo/+}$ mouse line. $VGAT^{floxneo/+}$ mice were crossed with CAG-Cre mice [14] to excise exons 2 and 3 (VGAT knockout allele), and $VGAT^{+/-}$ mice were obtained. We then intercrossed $VGAT^{+/-}$ mice to generate $VGAT^{-/-}$ mice. When we performed timed matings of the $VGAT^{+/-}$ mice, the morning on the day of vaginal plug detection was designated E0.5.

Genotypes of $VGAT^{+/+}$, $VGAT^{+/-}$ and $VGAT^{-/-}$ mice were determined by PCR using the following oligonucleotides: primer P1 (5'-AGTCTGATCCCGTGGCACTTCCAACTC-3') corresponding to intron 1 of the VGAT gene and primers P2 (5'-TCAGAGGCTTCT TCCTAGGGCTGCTG-3') and P3 (5'-GACCTCCCCCATTGCATAGAATGGCAC-3') corresponding to the 3'-flanking region of the VGAT gene. The primer set of P2 and P3 amplified a 183-bp fragment specific for the wild-type allele, and the primer set of P1 and P3 yielded a 430-bp fragment specific for the knockout allele.

GAD67 knockout mice

We used homozygous GAD67-GFP (□neo) ($GAD67^{GFP/GFP}$) mice as GAD67 knockout ($GAD67^{-/-}$) mice. The generation of the GAD67-GFP (□neo) mice and their genotyping by PCR were described previously [47,48]. In the GAD67-GFP (□neo) mice, a cDNA encoding enhanced green fluorescent protein (EGFP) followed by an SV40 polyadenylation signal was targeted to the locus encoding GAD67 by homologous recombination, and the GAD67 gene was disrupted.

Western blotting and measurement of neurotransmitter contents

For Western blotting, homogenates prepared from E18.5 mouse brain were separated by 7.5% SDS-polyacrylamide gel electrophoresis, transferred to nitrocellulose membrane (Whatman, Maidstone, UK), and probed with antibodies specific for VGAT (1:1000) [49], GAD65/67 (1:1000) [50], synaptophysin (1:1000) (Synaptic Systems, Goettingen, Germany), and β-actin (1:10000) (Abcam, Cambridge, UK). After the membranes were washed with Tris-HCl buffered saline containing 0.05% (w/v) Tween 20, the bound antibodies were visualized with horseradish peroxidase-conjugated goat anti-mouse IgG or anti-rabbit IgG (Jackson ImmunoResearch Laboratories, West Grove, PA) using the ECL Western blotting detection system (GE Healthcare, London, UK). Protein levels were quantified using Light Capture and its quantification software (ATTO, Tokyo, Japan). Expression levels were normalized to β-actin or synaptophysin levels, and the values are expressed as means ± SE. Statistical significance was assessed using Student's *t*-test.

GABA, glycine, and glutamate contents in the E18.5 mouse forebrain were measured according to previously described method [21,47].

Electrophysiological recording in spinal cord

Embryos (E17.5, 18.5) of control ($VGAT^{+/+}$; n = 3, $VGAT^{+/-}$; n = 5) and $VGAT^{-/-}$ (n = 12) mice were

decapitated and eviscerated, and the spinal cord was removed by ventral laminectomy. The isolated spinal cord was placed in a recording chamber perfused with oxygenated Ringer's solution (118.4 mM NaCl, 3 mM KCl, 2.52 mM $CaCl_2$, 1.25 mM $MgSO_4$, 25 mM $NaHCO_3$, 1.18 mM KH_2PO_4, and 11.1 mM D-glucose aerated with 5% CO_2 in O_2) at room temperature. Recordings from MNs in the isolated spinal cord were performed as described previously [17]. Briefly, visually guided whole-cell tight-seal recording of MNs was performed with patch electrodes pulled from thick walled borosilicate glass to a final resistance of 5-8 MΩ. The electrode tips were filled with (in mM) 138 K-gluconate, 10 HEPES, 1 $CaCl_2$, 5 ATP-Mg, and 0.3 GTP-Li. Intracellular signals were amplified with a Multiclamp 700B amplifier (Molecular Devices, Union City, CA), digitized at 5 kHz with the Digidata 1440A data acquisition system (Molecular Devices) and saved on a hard disk for off-line analysis. Electrical stimulations of lumbar ventral roots (VRs) were performed using glass suction electrodes. MNs were identified visually as cells with large soma in the ventral horn and by observing the antidromic firing activated by the electrical stimulation of the adjacent VR. All drugs (CNQX, AP5, strychnine and picrotoxin; Sigma-Aldrich, St. Louis, MO) were dissolved in Ringer's solution and bath-applied to the preparation. Analysis was performed using pClamp 10 software (Molecular Devices).

Histology

$VGAT^{-/-}$, $VGAT^{+/-}$ and $VGAT^{+/+}$ mice at E18.5 were investigated. Samples were fixed in 10% (vol/vol) formaldehyde, dehydrated with a graded series of ethanol solutions, and embedded in paraffin. Three-micrometer sections were prepared, subjected to paraffin removal by immersion in xylene, rehydrated, and stained with hematoxylin-eosin. $VGAT^{+/-}$ and $VGAT^{+/+}$ mice were mixed together and are referred to as control mice.

Additional material

Additional file 1: Supplementary Figure S1. VGAT expression levels in VGAT mutant mice. (A, B) VGAT expression level was normal in adult $VGAT^{floxneo/floxneo}$ mice. Western blot of whole brain homogenates from adult $VGAT^{+/+}$ (+/+) and $VGAT^{floxneo/floxneo}$ (floxneo/floxneo) mice is shown (A). VGAT expression level normalized to β-actin was not different between $VGAT^{+/+}$ (+/+) and $VGAT^{floxneo/floxneo}$ (floxneo/floxneo) mice (B). (C, D) VGAT expression level was reduced by about half in adult $VGAT^{+/-}$ mice. Western blot of whole brain homogenates of adult $VGAT^{+/+}$ (+/+) and $VGAT^{+/-}$ (+/-) mice is shown (C). VGAT expression level normalized to synaptophysin was significantly different between $VGAT^{+/+}$ (+/+) and $VGAT^{+/-}$ (+/-) mice (D). Significance was tested by Student's t-test (*P < 0.05).

Acknowledgements

The authors thank Ms. Honma, Ms. Hara and Ms. Yamazaki for technical assistance, and Ms. Shimoda and Ms. Owada for secretarial assistance. We thank Drs. Iso and Kurabayashi for the experiments and helpful discussion. We also thank the staff at the Institute of Experimental Animal Research, Gunma University Graduate School of Medicine for technical help. This study was supported by Grants-in-Aid for Scientific Research from the Ministry of Education, Culture, Sports, Science and Technology (MEXT) of Japan, a grant from the Co-operative Study Program of National Institute for Physiological Sciences, Japan, Research for Promoting Technological Seeds, and Takeda Science Foundation.

Author details

[1]Department of Genetic and Behavioral Neuroscience, Gunma University Graduate School of Medicine, Maebashi 371-8511, Japan. [2]The Graduate University for Advanced Studies, Hayama, Kanagawa 240-0193, Japan. [3]Japan Science and Technology Agency, CREST, Tokyo 102-0075, Japan. [4]Department of Pathology, Institute of Development, Aging and Cancer, Tohoku University, Sendai 980-8575, Japan. [5]Graduate School of Comprehensive Human Science, University of Tsukuba, Tsukuba 305-8577, Japan. [6]Department of Physiology, Hamamatsu University School of Medicine, Hamamatsu 431-3192, Japan. [7]Department of Human Pathology, Gunma University Graduate School of Medicine, Maebashi 371-8511, Japan. [8]Doshisha University Faculty of Life and Medical Sciences, Kyotanabe, Kyoto 610-0394, Japan. [9]Department of Cellular Neurobiology, Graduate School of Medicine, University of Tokyo, Tokyo 113-0033, Japan. [10]Department of Materials Science, Toyohashi University of Technology, Toyohashi 441-8580, Japan. [11]Department of Molecular Neurobiology and Pharmacology, Graduate School of Medicine, University of Tokyo, Tokyo 113-0033, Japan. [12]Division of Stem Cell Regulation Research, G6, Osaka University Graduate School of Medicine, 2-2 Yamadaoka, Suita, Osaka, 565-0871, Japan. [13]Mitsubishi Kagaku Institute of Life Sciences, MITILS, 11 Minamiooya, Machida, Tokyo, 194-8511, Japan. [14]Obata Research Unit, RIKEN Brain Science Institute, Wako 351-0198, Japan.

Authors' contributions

Conceived and designed the experiments: KS, TK, HN, YN, MY, SK, AF, MF, KN, KO, YY. Performed the experiments: KS, TK, HN, TF, RH, ST, SE, MU, KI, MF, KN, KO, YY. Analyzed the data: KS, TK, HN, TF, RH, KI, AF, MF, KN, KO, YY. Contributed new reagents/analytical tools: ST, MM, JM. Wrote the paper: KS, TK, HN, AF, MF, KN, KO, YY. All authors read and approved the final manuscript.

Competing interests

The authors declare that they have no competing interests.

Received: 26 November 2010 Accepted: 30 December 2010
Published: 30 December 2010

References

1. Roberts E, Kuriyama K: **Biochemical-physiological correlations in studies of the gamma-aminobutyric acid system.** *Brain Res* 1968, **8**:1-35.
2. McIntire SL, Reimer RJ, Schuske K, Edwards RH, Jorgensen EM: **Identification and characterization of the vesicular GABA transporter.** *Nature* 1997, **389**:870-876.
3. Sagne C, El Mestikawy S, Isambert MF, Hamon M, Henry JP, Giros B, Gasnier B: **Cloning of a functional vesicular GABA and glycine transporter by screening of genome databases.** *FEBS Lett* 1997, **417**:177-183.
4. Bu DF, Erlander MG, Hitz BC, Tillakaratne NJ, Kaufman DL, Wagner-McPherson CB, Evans GA, Tobin AJ: **Two human glutamate decarboxylases, 65-kDa GAD and 67-kDa GAD, are each encoded by a single gene.** *Proc Natl Acad Sci USA* 1992, **89**:2115-2119.
5. Esclapez M, Tillakaratne NJ, Kaufman DL, Tobin AJ, Houser CR: **Comparative localization of two forms of glutamic acid decarboxylase and their mRNAs in rat brain supports the concept of functional differences between the forms.** *J Neurosci* 1994, **14**:1834-1855.
6. Stork O, Ji FY, Kaneko K, Stork S, Yoshinobu Y, Moriya T, Shibata S, Obata K: **Postnatal development of a GABA deficit and disturbance of neural functions in mice lacking GAD65.** *Brain Res* 2000, **865**:45-58.
7. Kubo K, Nishikawa K, Ishizeki J, Hardy-Yamada M, Yanagawa Y, Saito S: **Thermal hyperalgesia via supraspinal mechanisms in mice lacking glutamate decarboxylase 65.** *J Pharmacol Exp Ther* 2009, **331**:162-169.
8. Asada H, Kawamura Y, Maruyama K, Kume H, Ding RG, Kanbara N, Kuzume H, Sanbo M, Yagi T, Obata K: **Cleft palate and decreased brain gamma-aminobutyric acid in mice lacking the 67-kDa isoform of glutamic acid decarboxylase.** *Proc Natl Acad Sci USA* 1997, **94**:6496-6499.

9. Dumoulin A, Rostaing P, Bedet C, Lévi S, Isambert MF, Henry JP, Triller A, Gasnier B: **Presence of the vesicular inhibitory amino acid transporter in GABAergic and glycinergic synaptic terminal boutons.** *J Cell Sci* 1999, 112:811-823.
10. Wojcik SM, Katsurabayashi S, Guillemin I, Friauf E, Rosenmund C, Brose N, Rhee JS: **A shared vesicular carrier allows synaptic corelease of GABA and glycine.** *Neuron* 2006, 50:575-587.
11. Aubrey KR, Rossi FM, Ruivo R, Alboni S, Bellenchi GC, Le Goff A, Gasnier B, Supplisson S: **The transporters GlyT2 and VIAAT cooperate to determine the vesicular glycinergic phenotype.** *J Neurosci* 2007, 27:6273-6281.
12. Saito K, Nakamura K, Kakizaki T, Ebihara S, Uematsu M, Takamori S, Yokoyama M, Konishi S, Mishina M, Miyazaki JI, Obata K, Yanagawa Y: **Generation and analysis of vesicular GABA transporter knockout mouse [abstract].** *Neurosci Res* 2006, 55:S80.
13. Ebihara S, Obata K, Yanagawa Y: **Mouse vesicular GABA transporter gene: genomic organization, transcriptional regulation and chromosomal localization.** *Brain Res Mol Brain Res* 2003, 110:126-139.
14. Sakai K, Miyazaki J: **A transgenic mouse line that retains Cre recombinase activity in mature oocytes irrespective of the cre transgene transmission.** *Biochem Biophys Res Commun* 1997, 237:318-324.
15. Wang YM, Gainetdinov RR, Fumagalli F, Xu F, Jones SR, Bock CB, Miller GW, Wightman RM, Caron MG: **Knockout of the vesicular monoamine transporter 2 gene results in neonatal death and supersensitivity to cocaine and amphetamine.** *Neuron* 1997, 19:1285-1296.
16. de Castro BM, De Jaeger X, Martins-Silva C, Lima RD, Amaral E, Menezes C, Lima P, Neves CM, Pires RG, Gould TW, Welch I, Kushmerick C, Guatimosim C, Izquierdo I, Cammarota M, Rylett RJ, Gomez MV, Caron MG, Oppenheim RW, Prado MA, Prado VF: **The vesicular acetylcholine transporter is required for neuromuscular development and function.** *Mol Cell Biol* 2009, 29:5238-5250.
17. Nishimaru H, Restrepo CE, Ryge J, Yanagawa Y, Kiehn O: **Mammalian motor neurons corelease glutamate and acetylcholine at central synapses.** *Proc Natl Acad Sci USA* 2005, 102:5245-5249.
18. Toribio RE, Brown HA, Novince CM, Marlow B, Hernon K, Lanigan LG, Hildreth BE, Werbeck JL, Shu ST, Lorch G, Carlton M, Foley J, Boyaka P, McCauley LK, Rosol TJ: **The midregion, nuclear localization sequence, and C terminus of PTHrP regulate skeletal development, hematopoiesis, and survival in mice.** *FASEB J* 2010, 24:1947-1957.
19. Yoda E, Hachisu K, Taketomi Y, Yoshida K, Nakamura M, Ikeda K, Taguchi R, Nakatani Y, Kuwata H, Murakami M, Kudo I, Hara S: **Mitochondrial dysfunction and reduced prostaglandin synthesis in skeletal muscle of Group VIB Ca2+-independent phospholipase A2gamma-deficient mice.** *J Lipid Res* 2010, 51:3003-3015.
20. Brewer S, Williams T: **Finally, a sense of closure? Animal models of human ventral body wall defects.** *Bioessays* 2004, 26:1307-1321.
21. Fujii M, Arata A, Kanbara-Kume N, Saito K, Yanagawa Y, Obata K: **Respiratory activity in brainstem of fetal mice lacking glutamate decarboxylase 65/67 and vesicular GABA transporter.** *Neuroscience* 2007, 146:1044-1052.
22. Baertschi S, Zhuang L, Trueb B: **Mice with a targeted disruption of the Fgfrl1 gene die at birth due to alterations in the diaphragm.** *FEBS J* 2007, 274:6241-6253.
23. Condie BG, Bain G, Gottlieb DI, Capecchi MR: **Cleft palate in mice with a targeted mutation in the gamma-aminobutyric acid-producing enzyme glutamic acid decarboxylase 67.** *Proc Natl Acad Sci USA* 1997, 94:11451-11455.
24. McIntire SL, Jorgensen E, Horvitz HR: **Genes required for GABA function in Caenorhabditis elegans.** *Nature* 1993, 364:334-337.
25. Aragon C, Lopez-Corcuera B: **Structure, function and regulation of glycine neurotransporters.** *Eur J Pharmacol* 2003, 479:249-262.
26. Conti F, Minelli A, Melone M: **GABA transporters in the mammalian cerebral cortex: localization, development and pathological implications.** *Brain Res Brain Res Rev* 2004, 45:196-212.
27. Cherubini E, Conti F: **Generating diversity at GABAergic synapses.** *Trends Neurosci* 2001, 24:155-162.
28. Schousboe A: **Role of astrocytes in the maintenance and modulation of glutamatergic and GABAergic neurotransmission.** *Neurochem Res* 2003, 28:347-352.
29. Sato K, Yoshida S, Fujiwara K, Tada K, Tohyama M: **Glycine cleavage system in astrocytes.** *Brain Res* 1991, 567:64-70.
30. Nishimaru H, Iizuka M, Ozaki S, Kudo N: **Spontaneous motoneuronal activity mediated by glycine and GABA in the spinal cord of rat fetuses in vitro.** *J Physiol* 1996, 497:131-143.
31. Hanson MG, Landmesser LT: **Characterization of the circuits that generate spontaneous episodes of activity in the early embryonic mouse spinal cord.** *J Neurosci* 2003, 23:587-600.
32. Sandri M, Carraro U: **Apoptosis of skeletal muscles during development and disease.** *Int J Biochem Cell Biol* 1999, 31:1373-1390.
33. Proske U, Morgan DL: **Muscle damage from eccentric exercise: mechanism, mechanical signs, adaptation and clinical applications.** *J Physiol* 2001, 537:333-345.
34. Liu J, Liu J, Mao J, Yuan X, Lin Z, Li Y: **Caspase-3-mediated cyclic stretch-induced myoblast apoptosis via a Fas/FasL-independent signaling pathway during myogenesis.** *J Cell Biochem* 2009, 107:834-844.
35. Williams T: **Animal models of ventral body wall closure defects: a personal perspective on gastroschisis.** *Am J Med Genet C Semin Med Genet* 2008, 148C:186-191.
36. Hubner CA, Stein V, Hermans-Borgmeyer I, Meyer T, Ballanyi K, Jentsch TJ: **Disruption of KCC2 reveals an essential role of K-Cl cotransport already in early synaptic inhibition.** *Neuron* 2001, 30:515-524.
37. Delpire E: **Cation-Chloride Cotransporters in Neuronal Communication.** *News Physiol Sci* 2000, 15:309-312.
38. Homanics GE, DeLorey TM, Firestone LL, Quinlan JJ, Handforth A, Harrison NL, Krasowski MD, Rick CE, Korpi ER, Makela R, Brilliant MH, Hagiwara N, Ferguson C, Snyder K, Olsen RW: **Mice devoid of gamma-aminobutyrate type A receptor beta3 subunit have epilepsy, cleft palate, and hypersensitive behavior.** *Proc Natl Acad Sci USA* 1997, 94:4143-4148.
39. Tsunekawa N, Arata A, Obata K: **Development of spontaneous mouth/tongue movement and related neural activity, and their repression in fetal mice lacking glutamate decarboxylase 67.** *Eur J Neurosci* 2005, 21:173-178.
40. Greer JJ, Funk GD: **Perinatal development of respiratory motoneurons.** *Respir Physiol Neurobiol* 2005, 149:43-61.
41. Suhren O, Bruyn GW, Tuynman JA: **Hyperexplexia - A Hereditary Startle Syndrome.** *J Neurol Sci* 1966, 3:577-605.
42. Zhou L, Chillag KL, Nigro MA: **Hyperekplexia: a treatable neurogenetic disease.** *Brain Dev* 2002, 24:669-674.
43. Ji F, Kanbara N, Obata K: **GABA and histogenesis in fetal and neonatal mouse brain lacking both the isoforms of glutamic acid decarboxylase.** *Neurosci Res* 1999, 33:187-194.
44. Kawaguchi Y, Kondo S: **Parvalbumin, somatostatin and cholecystokinin as chemical markers for specific GABAergic interneuron types in the rat frontal cortex.** *J Neurocytol* 2002, 31:277-287.
45. Ascoli GA, Alonso-Nanclares L, Anderson SA, Barrionuevo G, Benavides-Piccione R, Burkhalter A, Buzsáki G, Cauli B, Defelipe J, Fairén A, Feldmeyer D, Fishell G, Fregnac Y, Freund TF, Gardner D, Gardner EP, Goldberg JH, Helmstaedter M, Hestrin S, Karube F, Kisvárday ZF, Lambolez B, Lewis DA, Marin O, Markram H, Muñoz A, Packer A, Petersen CC, Rockland KS, Rossier J, Rudy B, Somogyi P, Staiger JF, Tamas G, Thomson AM, Toledo-Rodriguez M, Wang Y, West DC, Yuste R: **Petilla terminology: nomenclature of features of GABAergic interneurons of the cerebral cortex.** *Nat Rev Neurosci* 2008, 9:557-568.
46. Yanagawa Y, Kobayashi T, Ohnishi M, Kobayashi T, Tamura S, Tsuzuki T, Sanbo M, Yagi T, Tashiro F, Miyazaki J: **Enrichment and efficient screening of ES cells containing a targeted mutation: the use of DT-A gene with the polyadenylation signal as a negative selection maker.** *Transgenic Res* 1999, 8:215-221.
47. Tamamaki N, Yanagawa Y, Tomioka R, Miyazaki J, Obata K, Kaneko T: **Green fluorescent protein expression and colocalization with calretinin, parvalbumin, and somatostatin in the GAD67-GFP knock-in mouse.** *J Comp Neurol* 2003, 467:60-79.
48. Kaneko K, Tamamaki N, Owada H, Kakizaki T, Kume N, Totsuka M, Yamamoto T, Yawo H, Yagi T, Obata K, Yanagawa Y: **Noradrenergic excitation of a subpopulation of GABAergic cells in the basolateral amygdala via both activation of nonselective cationic conductance and suppression of resting K+ conductance: a study using glutamate decarboxylase 67-green fluorescent protein knock-in mice.** *Neuroscience* 2008, 157:781-797.
49. Takamori S, Riedel D, Jahn R: **Immunoisolation of GABA-specific synaptic vesicles defines a functionally distinct subset of synaptic vesicles.** *J Neurosci* 2000, 20:4904-4911.

50. Asada H, Kawamura Y, Maruyama K, Kume H, Ding R, Ji FY, Kanbara N, Kuzume H, Sanbo M, Yagi T, Obata K: Mice lacking the 65 kDa isoform of glutamic acid decarboxylase (GAD65) maintain normal levels of GAD67 and GABA in their brains but are susceptible to seizures. *Biochem Biophys Res Commun* 1996, 229:891-895.

doi:10.1186/1756-6606-3-40
Cite this article as: Saito *et al.*: The physiological roles of vesicular GABA transporter during embryonic development: a study using knockout mice. *Molecular Brain* 2010 3:40.

Behavioral/Systems/Cognitive

X11-Like Protein Deficiency Is Associated with Impaired Conflict Resolution in Mice

Yoshitake Sano,[1] Veravej G. Ornthanalai,[2] Kazuyuki Yamada,[3] Chihiro Homma,[3] Hitomi Suzuki,[1] Toshiharu Suzuki,[4] Niall P. Murphy,[2] and Shigeyoshi Itohara[1]

[1]Laboratory for Behavioral Genetics, [2]Molecular Neuropathology Group, and [3]Research Resource Center, RIKEN Brain Science Institute, Wako, Saitama 351-0198, Japan, and [4]Laboratory of Neuroscience, Graduate School of Pharmaceutical Sciences, Hokkaido University, Sapporo, Hokkaido 060-0812, Japan

Understanding how emotion is generated, how conflicting emotions are regulated, and how emotional states relate to sophisticated behaviors is a crucial challenge in brain research. Model animals showing selective emotion-related phenotypes are highly useful for examining these issues. Here, we describe a novel mouse model that withdraws in approach-avoidance conflicts. X11-like (X11L)/Mint2 is a neuronal adapter protein with multiple protein-protein interaction domains that interacts with several proteins involved in modulating neuronal activity. X11L-knock-out (KO) mice were subordinate under competitive feeding conditions. X11L-KO mice lost significantly more weight than cohoused wild-type mice without signs of decreased motivation to eat or physical weakness. In a resident-intruder test, X11L-KO mice showed decreased intruder exploration behavior. Moreover, X11L-KO mice displayed decreased marble-burying, digging and burrowing behaviors, indicating aberrant ethological responses to attractive stimuli. In contrast, X11L-KO mice were indistinguishable from wild-type mice in the open field, elevated plus maze, and light/dark transition tests, which are often used to assess anxiety-like behavior. Neurochemical analysis revealed a monoamine imbalance in several forebrain regions. The defective ethological responses and social behaviors in X11L-KO mice were rescued by the expression of X11L under a *Camk2a* promoter using the Tet-OFF system during development. These findings suggest that X11L is involved in the development of neuronal circuits that contribute to conflict resolution.

Introduction

Behavior arises from the integration of multiple emotional processes, which may themselves conflict. Approach-avoidance conflict in response to various emotional stimuli (e.g., seeking friendship, overcoming shyness or desiring success, avoiding competition) is a common everyday experience. Studies of human genetics and genetically engineered mice have gradually begun to unravel the molecular and neuronal mechanisms underlying emotion-related behavior, and cumulative evidence supports a crucial role of monoaminergic systems (Lesch et al., 1996; Zhuang et al., 1999; Gross et al., 2002; Finn et al., 2003; Holmes et al., 2003; Reif and Lesch, 2003). Behavioral paradigms designed to assess anxiety-related behaviors are relatively well established. In many of these paradigms, anxiety-like behavior is inferred by the avoidance of unpleasant stimuli under conflicting situations. However, more sophisticated paradigms and model animals that allow us to distinguish various emotional states are required to clarify how conflicting emotions are regulated in the brain and how emotional states underlie behavior.

The neuronal adaptor protein X11L (also called X11β and Munc18–1 interacting protein 2; Mint2) interacts with amyloid precursor protein (APP) and regulates APP metabolism (Tomita et al., 1999; Araki et al., 2003; Lee et al., 2004; Sano et al., 2006a; Saito et al., 2008). X11L suppresses amyloidogenic processing of APP via intracellular sorting machinery, and thus the lack of X11L in mice is associated with an increase in amyloid β (Aβ) 40 and 42 in the hippocampus (Sano et al., 2006a). X11L constitutes the X11 protein family with X11/X11α/Mint1 and X11L2/X11γ/Mint3, which comprises a poorly conserved N-terminal region, a conserved central phosphotyrosine interaction domain, and two C-terminal PDZ [postsynaptic density-95/*Drosophila* disks-large/zona occludens-1] domains (Tomita et al., 1999). X11L and X11 are brain-specific proteins that interact with many molecules, such as Munc18–1, calcium channels, β-neurexin, and hyperpolarization-activated cyclic nucleotide-gated potassium channel 2, involved in the regulation of neuronal/synaptic activity (Okamoto and Südhof, 1997; Maximov et al., 1999; Tomita et al., 1999; Biederer and Südhof, 2000; Kimura et al., 2004; Rogelj et al., 2006). Approximately 80% of Mint1/2 (X11/X11L) double-knock-out (KO) mice, but not single-gene KO mice, die at birth, and presynaptic release probability is decreased in the hippocampal excitatory neurons of double-KO mice, but not Mint1 (X11) single-KO mice (Ho et al., 2003, 2006), indicating substantial redundancies between X11 and X11L functions. The physiological roles of X11L, however, are not well understood.

Received Dec. 3, 2008; revised March 12, 2009; accepted April 4, 2009.

This work is supported in part by a Grant-in-Aid for Young Scientists (B) from Japan Society for the Promotion of Science 18700403 to Y.S. We thank Chadwick Boulay for preliminary neurochemical analyses, Sam Gandy for the G369 antibody, Takayuki Sassa for the NLS-LacZ plasmid, Hidenori Taru for the FLAG-hX11L plasmid, and the staff of the RIKEN Brain Science Institute animal facility for their commitment to maintaining animals and preparing the behavioral apparatuses. We also thank all of our colleagues in our laboratories for their encouragement and discussions.

Correspondence should be addressed to Shigeyoshi Itohara, Laboratory for Behavioral Genetics, RIKEN BSI, 2-1 Hirosawa, Wako 351-0198, Japan. E-mail: sitohara@brain.riken.jp.

DOI:10.1523/JNEUROSCI.5756-08.2009

 0270-6474/09/295884-13$15.00/0

Here, we performed studies to identify the neuronal mechanisms regulated by X11L and to determine whether X11L-KO mice could model Alzheimer's disease (AD). Thus, we extensively analyzed the behavioral phenotypes, and neurochemical and neurophysiological characteristics of X11L-KO mice. Although no deficits in learning, memory, or synaptic properties were detected in X11L-KO mice, we observed characteristic deficits in motivated approach behaviors associated with emotional conflict. Restoration of expression of X11L during development restored normal performance in the resident-intruder and ethological tests designed to observe species-typical behaviors to attractive stimuli, such as unfamiliar-objects/thick-bedding and a clogged-tunnel. We suggest that X11L-KO mice provide a unique opportunity to address the neuronal mechanisms that underlie emotional conflict.

Materials and Methods

Animals

All experimental protocols were approved by the Animal Care and Use Committees of the RIKEN Brain Science Institute. X11L-KO mice were previously generated as a C57BL/6 coisogenic strain (Sano et al., 2006a). A tTA transgenic mouse line, B6;CBA-Tg(Camk2a-tTA)1Mmay/J, under control of the *Camk2a* promoter (Mayford et al., 1996), was obtained from The Jackson Laboratory. The constructs of *FLAG-humanX11L (hX11L)* (Taru and Suzuki, 2004) and *NLS-LacZ* (Sassa et al., 2004) have been described previously. These coding sequences together with splicing signals derived from the pMSG vector (GE Healthcare) were inserted downstream from the bidirectional tet-response element (TRE)-dependent promoters of the pBI Tet vector (Clontech). The resulting *FLAG-X11L-TRE-NLS-LacZ* construct was microinjected into fertilized C57BL/6 eggs. The generated mouse lines were crossed with *Camk2a-tTA* mice. We selected a representative line that bidirectionally expressed FLAG-X11L and NLS-LacZ at the highest level depending on the presence or absence of doxycycline (DOX) (Sigma-Aldrich).

Experimental groups of wild-type (WT) and X11L-KO mice were generated by intercrossing X11L heterozygous mutant mice. To obtain *FLAG-X11L-TRE-NLS-LacZ/Camk2a-tTA* double-transgenic (DTg) mice under the X11L-KO background (DTg:X11L-KO mice), we first generated each single-transgenic mouse under the X11L-KO background and intercrossed them. X11L-KO littermates from the crosses were used for the behavioral studies. These mice theoretically carry 99% or more of the C57BL/6-derived genome. Genetic background-matched and age-matched WT mice were obtained independently from crosses between X11L-mutation heterozygotes of the same generation.

Adult male mice >3 months old were used. Mice were maintained under a 12 h light and dark cycle (lights on, 8:00 A.M.–8:00 P.M.), and *ad libitum* feeding and drinking conditions. Mice were group-housed by combining equal numbers of each genotype, unless otherwise stated. An investigator ignorant to the genotype of the animals performed all behavioral, pharmacological, and electrophysiological experiments.

Antibodies

The mouse monoclonal anti-X11L C-terminal domain (347–5) was described previously (Sumioka et al., 2003). Anti-Mint2/X11L (611033) was purchased from BD Biosciences; horseradish peroxidase (HRP)-conjugated anti-β-tubulin (s.c.-9104) was from Santa Cruz Biotechnology; anti-FLAG M2 (F1804) was from Sigma-Aldrich; anti-galactosidase (55976) was obtained from Cappel Laboratories; and HRP-conjugated anti-mouse IgG (NA931) and HRP-conjugated anti-rabbit IgG (NA934) were purchased from GE Healthcare.

Western blotting analysis

Western blotting was performed as described previously (Sano et al., 2006a,b). Details are described in the supplemental materials, available at www.jneurosci.org.

Behavioral analysis

Competitive food restriction. Groups of mice were cohoused in the same cage for at least a week before food restriction. In mixed genotype housing cages, equal numbers of WT and X11L-KO mice [(2 + 2) or (3 + 3) per cage] were cohoused. In uniform genotype housing cages, genotype-matched mice (4–6 mice/cage) were cohoused. During the food restriction period, mice were provided with 2 or 3 food pellets, equivalent to 4% of their free-feeding body weight, per day. During all test periods, mice were allowed water *ad libitum*. Weight was measured daily before feeding.

Food intake. To examine food intake of the mice under noncompetitive conditions, mice that were food-restricted as described above in mixed genotype housing cages were housed individually and then fed *ad libitum* for 90 min. The amount of food consumed and weight-gain after feeding was measured. Calculated food intake and weight-gain were normalized to the body weight measured before feeding.

Grip strength. A spring balance attached to the distal end of a wire-mesh end was used to test grip strength (O'Hara & Co.). Mice were allowed to grip the wire-mesh with their forelimbs, and were then pulled gently in a horizontal direction by their tails, away from the spring balance. The force applied to the spring balance at the moment the mice released the wire-mesh was recorded. Measurements were repeated twice with a 30 min intertrial interval. The mean of the two trials was calculated. In this test, mice were normally housed without food restriction.

Resident-intruder test. The resident-intruder test was performed according to the procedure described previously (Wada et al., 1997). Resident mice were maintained in individual housing at least for 5 weeks before experimentation. Corn cob (GreenTru; Green Products Company) was used for the bedding material to allow for easy observation of the mouse behavior. Intruder mice (male, DBA/2J strain; JCL Inc.; 7 weeks) were housed in groups of 4–5 mice per cage with standard bedding material (Tek-Fresh; Harlan) for 2 weeks before the experiment.

In the resident-intruder test, residents' cages were placed in an area with low lighting (120 lux). The intruder was transferred to the resident home cage, then social behaviors of the resident mouse toward the intruder mouse were observed for 5 min. The test was conducted twice (24 h intertrial interval) using different intruder mice for each trial. The following behavioral indices were measured. Approaching: exploratory behavior toward the intruder, sometimes involving contact with the intruder and sniffing behavior; Following: exploratory following and chasing of the intruder; and Aggression: aggressive movements against the intruder, such as fighting, biting, and other aggressive responses (aggressive-sniffing, -grooming, -following). As some indices may or may not involve aggression, behaviors were counted as aggressive only when the intruder responded with a submissive posture (Grant and Mackintosh, 1963). Behaviors of the resident mice were analyzed and counted using commercial software (VideoStudio, Corel) after the experiment.

Marble burying test and digging test. The marble burying test (MBT) was performed according to the procedure described previously (Yamada et al., 2002) with some modifications. Twenty clear blue glass marbles (17 mm diameter), white paper bedding material (Paperclean; Japan SLC), and transparent cages (24 × 45 × 21 [H] cm) were used for each trial. The cage was filled with bedding (5 cm deep). Mice were individually habituated to the cages for 30 min (habituation session) and then returned to their home cages. The 20 glass marbles were placed on the bedding surface in the habituated cage, evenly spaced at 5 cm intervals. The mice were then placed into the same cages to which they were habituated (MBT session) and allowed to remain for 20 min. After 20 min, the mice were removed from the cage and the number of marbles buried more than two-thirds in the bedding was counted. In both the habituation and MBT sessions, horizontal and vertical activity of the mice was measured using a two-level infrared beam apparatus (Scanet, Melquest). In the digging test, the mice were placed on the bedding (5 cm deep) without any marbles present. Mouse behavior was recorded from above for 30 min using a video camera, and the time spent digging was measured manually.

Burrowing test. The burrowing test was performed according to previously described procedures (Deacon et al., 2002) with some modifications. Both WT and X11L-KO mice were maintained in individual housing. Two gray vinyl chloride tubes (inside tube diameter, 56 mm; length, 150 mm; open end of the tube raised 30 mm; lower end closed with a cap)

were placed in their home cage at ~3 h before the start of dark period. One tube was filled with 200 g of the usual food pellets, each weighing ~2 g, while other tube was empty to provide a shelter. The weight of displaced food pellets from the tube was weighed after a 15 h period.

Methods for the other behavioral tasks are described in the supplemental materials, available at www.jneurosci.org.

β-Galactosidase (LacZ) staining

LacZ staining was performed according to previously described procedure (Iwasato et al., 2000; Tanaka et al., 2008) with some modifications. Mice were deeply anesthetized with 2,2,2-tribromoethanol (Avertin, Sigma-Aldrich) and transcardially perfused with physiological saline and then 4% (w/v) paraformaldehyde in 0.1 M sodium phosphate buffer (PB), pH 7.4, at 4°C for 20 min. The brains were excised, postfixed with the same fixative at 4°C for 2 h, and equilibrated in 30% (w/v) sucrose in PB as a cryoprotectant. The brains were embedded in OCT compound (Sakura Finetech), and frozen sections (20 μm) were prepared. Sections were then washed in phosphate buffered saline (PBS) on ice for 5 min and stained in 1 mg/ml X-gal, 5 mM $K_3Fe(CN)_6$, 5 mM $K_4Fe(CN)_6$, 20 mM Tris/HCl pH 7.5, and 2 mM $MgCl_2$ in PB at 37°C overnight. LacZ-stained sections were washed in PBS and then counter-stained with eosin.

Monoamine measurement

Circular tissue punches (1 mm diameter) were taken from 150 μm thick frozen coronal brain sections obtained from 4- to 5-month-old mice ($n = 8$ per group) and stored at −80°C until assayed. Monoamines and metabolites were extracted by sonication in 0.1 M perchloric acid containing a mixture of internal standards (200 nM isoproterenol, 200 μM L-norleucine, and 5 μM ethylhomocholine). Protein was then measured using a DC Protein Assay kit (Bio-Rad). The remainder of the sample was centrifuged for 15 min at 15,000 rpm and the supernatant filtered through polyvinylidene fluoride 0.22 μm micropore filters (Millipore Corp.) by centrifugation (14,000 rpm for 5 min). The filtrate was analyzed by high pressure liquid chromatography coupled to electrochemical detection (Eicom). Briefly, an Eicompak SC-5ODS 3.0 × 150 mm column was used for separations, perfused with a mobile phase consisting of citrate (41.4 mM), sodium acetate (39.2 mM), methanol (17%), sodium 1-octanesulfonate (190 mg/L), and EDTA (5 mg/L), adjusted to pH 3.7 using glacial acetic acid and pumped at a rate of 0.5 ml/min. The working electrode (WE-3G) potential was set at +0.75 V. Column temperature was maintained at 25°C. Data were collected and analyzed by Ezchrom Elite software (Scientific Software Inc.). All analyte information, including the retention times, peak heights, concentrations, and recovery rate of internal standards, was calculated by comparison to standard curves generated for known concentrations of external standards that were run daily. Turnover rates were calculated as follows: noradrenaline (NA) turnover rate = [3-methoxy-4-hydroxyphenylglycol (MHPG)]/[NE]; dopamine (DA) turnover rate = [3, 4-dihydroxyphenylacetic acid (DOPAC)] + [homovanillic acid (HVA)]/[DA]; serotonin (5-HT) turnover rate = [5-hydroxyindoleacetic acid (5-HIAA)]/[5-HT]. Correlation maps were constructed using iVici software (Michnick Laboratory, http://michnick.bcm.umontreal.ca/ivici/) using correlation coefficients calculated by pairwise comparisons (Tarassov and Michnick, 2005).

8-Hydroxy-2-dipropylaminotetralin-induced hypothermia

(±)-8-Hydroxy-2-dipropylaminotetralin (8-OH-DPAT) hydrobromide was purchased from Tocris Bioscience. The 8-OH-DPAT induced hypothermia experiment was performed according to the procedure described previously (Li et al., 1999) with minor modifications. Mice were handled every day for 1 week before the experiment. Mouse body temperature was measured using a digital thermometer with a temperature probe (Physitemp BAT-12R and RET-3) inserted 2–2.5 cm into the rectum, with the mouse slightly restrained by the tail. WT and X11L-KO mice were subcutaneously injected with saline or 8-OH-DPAT at doses of 0.1 or 0.5 mg/kg. Body temperature was monitored every 10 min for 60 min before the injection and every 15 min for 90 min after the injection. Mean temperature before injection was used as the basal temperature.

Statistics

Statistical analyses were performed using SPSS 14.0J or Excel statistics 2008 (Social Survey Research Information Co.) software. For comparison of two groups in most experiments, we applied an unpaired two-tailed t test. A repeated measures ANOVA was used to analyze learning data through training from the water maze and radial maze tests, and the 2 d of data from the resident-intruder test. We used a single-factor ANOVA followed by Scheffe's *post hoc* analysis to test for differences among three or more independent groups. Nonparametric tests were used to analyze data from the marble buying, digging and burrowing tests (Mann–Whitney U test for comparison of two groups or Steel test for rescue experiments). Differences were considered to be statistically significant when the probability value was <0.05.

Results

X11L-KO mice do not exhibit an AD-model like phenotype in terms of learning and memory

Amyloid β40 and 42 levels are increased in X11L-KO mice (Sano et al., 2006a). Patients with AD as well as AD mouse models that exhibit Aβ accumulation are cognitively impaired (Chen et al., 2000; Janus et al., 2000; Morgan et al., 2000). To determine whether X11L-KO mice have an AD-like phenotype, we analyzed their learning and memory ability. The Morris water maze task is a hippocampus-dependent task that is most frequently used to detect dysfunction of learning and memory performance in mouse models of AD. Despite the increase in Aβ in X11L-KO hippocampi, the learning and memory performance of X11L-KO and WT mice was comparable (supplemental Fig. 1*A–C*, available at www.jneurosci.org as supplemental material). Working memory in the 8-arm radial maze test and associative memory in context-dependent and cue-dependent fear conditioning tests were not impaired in X11L-KO mice compared with WT mice (supplemental Fig. 1*D*,*E*, available at www.jneurosci.org as supplemental material). These data suggest that learning and memory functions in X11L-KO mice are largely intact.

An accumulation of Aβ may depress neuronal transmission (Chapman et al., 1999; Kamenetz et al., 2003). Additionally, X11L interacts with the synaptic machinery that regulates neurotransmitter release such as Munc 18–1 and β-neurexin (Okamoto and Südhof, 1997; Biederer and Südhof, 2000; Ho et al., 2003, 2006). Expression of X11L is most abundant in the CA3 pyramidal neurons (Nakajima et al., 2001). Thus, we next examined the synaptic properties of the CA3-CA1 synapse in hippocampal slices from WT and X11L-KO mice. Basal synaptic transmission, paired-pulse facilitation (a form of short-term plasticity), and long-term potentiation in slices from X11L-KO mice were similar to those of WT littermates (supplemental Fig. 2*A–C*, available at www.jneurosci.org as supplemental material). In the hippocampus, no differences were detected between X11L-KO and WT mice in the amounts of X11/X11L binding, or of the levels of presynaptic and postsynaptic molecules examined (supplemental Table 1, available at www.jneurosci.org as supplemental material).

Therefore, the behavioral and physiological data do not support the tenet that X11L-KO mice are AD-like animal model associated with dementia.

X11L-KO mice are subordinated by their WT peers under competitive conditions

We noticed that X11L-KO mice showed a unique behavioral phenotype during a set of repeated radial maze tests. When food restriction was implemented by limiting the amount of time during which food was available (90 min free feeding/d), group housed X11L-KO and WT mice had a similar rate of body weight loss. When the food restriction regimen was transiently shifted to

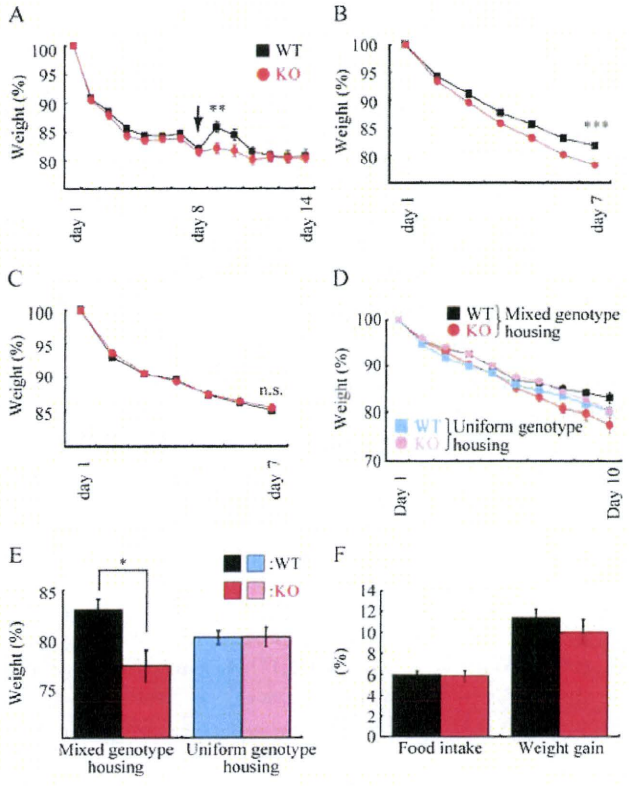

Figure 1. X11L-KO mice are subordinated in competitive feeding conditions. ***A–C***, The percentages of weight reduction by food deprivation for the mixed genotype housing condition (WT mice, black square; X11L-KO mice, red circle). Free-feeding body weight was defined as 100%. ***A***, From day 1 to day 7, mice could freely feed for 90 min per day. At day 8 (arrow), only an amount of food equivalent to 8% of the sum of the mouse body weight per cage was provided. ***B***, Food pellets (2 pellets/4 mice; amount of food = 4% of the sum of the mouse body weights per cage under free-feeding conditions) were placed into the cages from day 1 to 7. ***C***, Food was restricted by a time-limited manner of free feeding for 90 min/d. ***D***, The percentages of weight reduction by food deprivation are shown for 10 d under different housing conditions (WT mice in mixed genotype housing, black square; X11L-KO mice in mixed genotype housing, red circle; WT mice in uniform genotype housing, blue square: X11L-KO mice in uniform genotype housing, pink circle). Body weights in the *ad libitum* feeding condition were defined as 100%. ***E***, Percentage body weight at day 10 is shown. In only the mixed genotype housing, X11L-KO mice lost significantly more weight than did WT mice. ***F***, The percentage of food intake and weight gain during the 90 min free feeding after 11 d of competitive food restriction was the same between genotypes. Data represent mean ± SE. $*p < 0.05$; $**p < 0.01$; $***p < 0.001$. (WT mice, black and blue columns; X11L-KO mice, red, and pink columns).

restricting the amount of food available on day 8 (amount of food = 8% of the summed body weight per cage), WT mice had a transiently larger weight gain than cohoused X11L-KO mice (7–8 months old, $n = 12$ per group; at day 9, $p < 0.01$) (Fig. 1*A*). This differential weight loss in X11L-KO mice was reproduced in another experiment. X11L-KO mice lost significantly more weight than cohoused WT mice under the amount-limited (competitive) feeding regimen (amount food = 4% of the summed body weight per cage per day; 3–4 months old, $n = 12$ per group; at day 7, $p < 0.001$) (Fig. 1*B*). Under the time-limited (no or very low-competitive) condition (90 min free feeding per day), there were no differences in body weight between genotypes (8–9 months old, $n = 12$ per group, $p = 0.68$) (Fig. 1*C*).

Based on these observations, we hypothesized that X11L-KO mice were subordinated under competitive feeding conditions. To test this hypothesis, we restricted feeding using two types of group housing conditions: equal numbers of WT and X11L-KO mice per cage (referred to as "mixed genotype housing") or groups of a single genotype mice per cage (referred to as "uniform genotype housing"). To avoid the influence of body weight at the start, the WT and X11L-KO mice in the mixed genotype housing were weight matched. During 10 d of feeding restriction using the limited-amount regimen, the X11L-KO mice in the mixed genotype housing cages lost significantly more weight than the WT mice (5–6 months old, $n = 6$ per group; weight ratio at day 10; WT, 82.9 ± 1.14%; X11L-KO, 77.3 ± 1.56%). No differences between genotypes were induced by the same treatment in uniform genotype housing (weight ratio at day 10; WT, 80.2 ± 0.68%, $n = 5$; X11L-KO, 80.2 ± 0.97%, $n = 6$). ANOVA and *Post hoc* Scheffe's test revealed significant differences between genotypes only in the mixed genotype housing groups ($F_{(3,19)} = 4.05$, $p < 0.05$; Scheffe's test, WT vs X11L-KO in mixed genotype housing, $p < 0.05$; in uniform genotype housing, $p = 1.00$) (Fig. 1*D*,*E*).

To rule out the possibility that the larger weight loss in X11L-KO mice was caused by a loss of appetite, the amount of food ingested and of weight gain after eating were measured under noncompetitive conditions in which each food-deprived mice were fed individually. Food intake and weight gain in X11L-KO mice were indistinguishable from those of WT mice (3–4 months old, $n = 12$ per group; food intake, $p = 0.85$; weight gain, $p = 0.33$) (Fig. 1*F*). Lever-pressing behavior to obtain food pellets in an operant conditioning test, in which mice received a 20 mg pellet when they pressed the lever 1, 10, or 50 times, was not different between genotypes (data not shown). These data indicate that the weight loss in X11L-KO mice in the competitive condition was not likely caused by a decreased motivation to eat, or a reduction in the incentive value of the food.

We considered the possibility that X11L-KO mice were less able to access food when competing with WT mice due to a physical limitation, such as weaker muscle strength. We assessed muscle (grip) strength of the forelimbs of WT and X11L-KO mice, and observed no differences between genotypes (7–8 months old, $n = 24$ per group; WT, 0.71 ± 0.03 Newtons (N); X11L-KO, 0.80 ± 0.04 N; grip strength, $p = 0.08$). Moreover, neither X11L-KO nor WT mice had wounds consistent with aggressive behavior in the home cage. Together, these findings suggested that X11L-KO mice are subordinated only under highly competitive conditions, and that this response is not due to a physical factor.

X11L-KO mice exhibit reduced social interaction

Because the subordinate feeding behaviors of the X11L-KO mice were observed under competitive conditions, we hypothesized that X11L-KO might show aberrant social interaction. To assess social behavior in X11L-KO mice, we used the resident-intruder test. We measured nonaggressive approach and following, and aggressive behaviors against intruder mice (see experimental procedure for details). In our experiment, fighting behavior was rarely observed. Approaching and following behaviors were lower in resident X11L-KO mice compared with WT mice (5–6 months old, $n = 10$ per group; approach, $F_{(1,18)} = 4.27$, $p = 0.05$; following, $F_{(1,18)} = 4.43$, $p < 0.05$; aggression, $F_{(1,18)} = 1.59$, $p = 0.22$; Figure 2*A–C*). The total number of resident social interactions with intruder mice was significantly decreased in X11L-KO mice compared with WT mice ($F_{(1,18)} = 9.14$, $p < 0.01$) (Fig. 2*D*). These data indicate that social interaction is suppressed in X11L-KO mice.

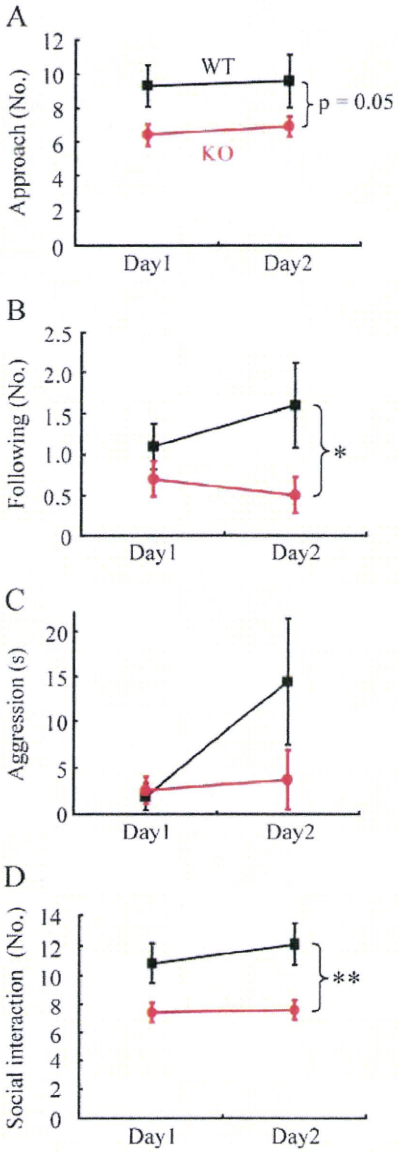

Figure 2. Social interaction against an intruder is significantly decreased in X11L-KO mice. ***A–C***, The resident-intruder test (WT mice, black square; X11L-KO mice, red circle) was performed for 2 consecutive days using different intruder mice for each trial. The numbers of approaches (***A***) and following behaviors (***B***) of resident mice against intruder mice were lower in X11L-KO mice. ***C***, Differences in the amount of time spent by resident mice exhibiting aggressive behavior in which the intruder mice showed a typical submissive pose was not statistically significant between genotypes. ***D***, The summed number of social interactions of resident mice toward intruder mice was significantly decreased in X11L-KO mice compared with WT mice. Data represent mean ± SE. $*p < 0.05$; $**p < 0.01$.

X11L-KO mice do not show altered anxiety-like behavior in conventional behavioral tests

Social interaction is the result of an inherent conflict in approach-avoidance factors, and is decreased under anxiogenic conditions (File, 1992; Crawley, 2007). Even if anxiety in the social interaction test qualitatively differs from that assessed on the elevated plus maze test, anxiolytic drugs are effective in both models (File, 1992; Nakamura and Kurasawa, 2001; Crawley, 2007). To gain insight into anxiety-related behaviors in X11L-KO mice, we subjected X11L-KO mice to open field, elevated plus maze, and light-dark transition tests. The behavior of the X11L-KO mice was comparable to that of WT mice in all of these tests (supplemental Table 2, available at www.jneurosci.org as supplemental material). Furthermore, X11L-KO mice did not show abnormalities in model behavioral tests for mental disorders such as the tail suspension test (a model of depression-like behavior) and prepulse inhibition test (a model for sensory motor gating activities associated with schizophrenia; supplemental Table 2, available at www.jneurosci.org as supplemental material). X11L-KO and WT mice showed comparable locomotor activity and circadian rhythms (supplemental Table 2, available at www.jneurosci.org as supplemental material). These results suggest that suppressed social interaction is not caused by enhanced anxiety-like, depressive behavior, or decreased locomotor activity.

X11L-KO mice show attenuated marble burying, digging, and burrowing behavior

The behavioral paradigms described above identify anxiety-related phenotypes based on avoidance behavior elicited by aversive stimuli. We examined whether behaviors that reflect approach motivation to some stimuli are selectively altered in X11L-KO mice. Behavior of X11L-KO mice and WT mice was therefore evaluated in the MBT. The MBT is proposed to be a model of defensive behavior, as mice actively bury glass marbles under a layer of bedding material (Broekkamp et al., 1986; Nicolas et al., 2006) (see also below). X11L-KO mice buried significantly fewer marbles than did WT mice (4–5 months old, $n = 12$ per group; WT, 11.2 ± 1.1; X11L-KO mice, 1.7 ± 0.76; number of buried marbles, $p < 0.001$) (Fig. 3*A*). Horizontal and vertical activity of X11L-KO mice was indistinguishable from that of WT mice in both the habituation and MBT sessions (locomotor activity in habituation session, $p = 0.75$; locomotor activity in MBT session, $p = 0.97$; rearing in habituating session, $p = 0.40$; rearing in MBT session, $p = 0.88$) (Fig. 3*B*,*C*). These data indicate that impaired marble burying behavior was not due to a reduction in general activity.

Marble burying behavior is argued to be the result of innate digging behavior (Njung'e and Handley, 1991a; Gyertyán, 1995; Deacon, 2006b). Thick bedding, which is used for the MBT, strongly motivates mice to dig the bedding material. This innate behavior is not habituated, is evoked in the absence of glass marbles, and continues even after all marbles are buried (Webster et al., 1981; Dudek et al., 1983; Gyertyán, 1995; Masuda et al., 2000; Deacon, 2006b). To assess whether impaired marble burying is associated with digging behavior, we measured the time spent digging during the habituation session. X11L-KO mice spent significantly less time digging (4–5 months old, $n = 12$ per group; WT, 288.9 ± 34.3 s; X11L-KO, 90.2 ± 15.3 s; $p < 0.001$) (Fig. 3*D*). Digging behavior was initiated within the first 10 min under conditions of a novel environment with thick bedding materials (supplemental Fig. 3*A*, available at www.jneurosci.org as supplemental material). In an independent experiment, strong and compulsive digging behavior was induced by bedding materials in the absence of marbles, depending on the bedding thickness (supplemental Fig. 3*B*, available at www.jneurosci.org as supplemental material). In this condition, X11L-KO mice again exhibited significantly reduced digging behavior. These data suggest that marble burying and digging behaviors are closely associated, and that the approach behavior motivated by incentives, such as marbles and bedding materials, is attenuated in X11L-KO mice.

Burying and digging behaviors are species-typical behaviors to some rodents. The burrowing test is conceptually related to the above ethological tests, as mice typically burrow

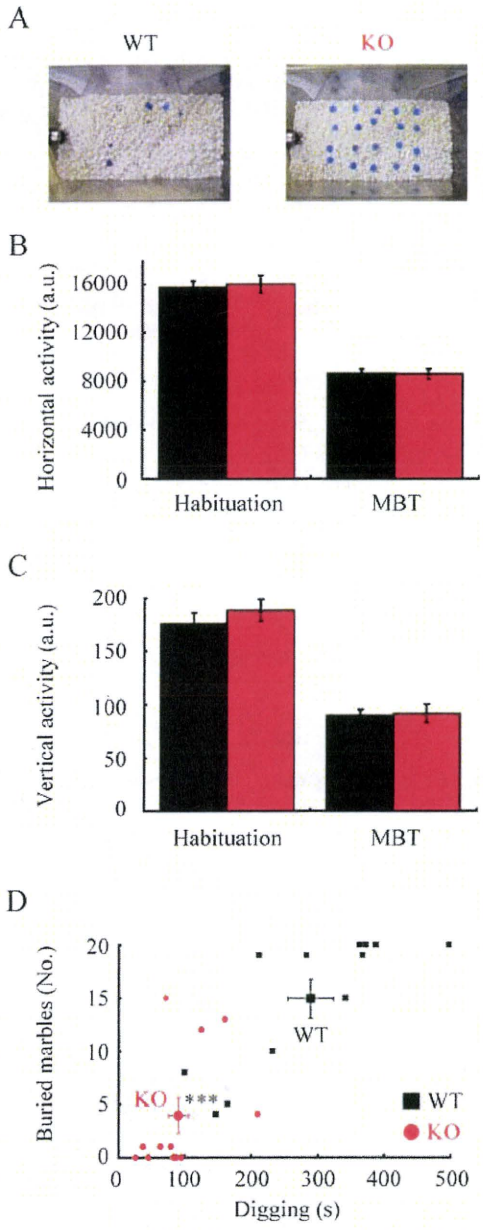

Figure 3. Marble burying and digging behaviors are impaired in X11L-KO mice. ***A***, Typical images of the cage after the marble burying test are shown. ***B***, ***C***, Horizontal (***B***) and vertical (***C***) activity in the habituation and MBT sessions was not significantly different in X11L-KO mice compared with WT mice. ***D***, The number of marbles buried and time spent digging during the habituation session (30 min) are plotted for each mouse. Data represent mean ± SE. ***$p <$ 0.001 (WT mice, black column; X11L-KO mice, red column).

into tunnel-like containers filled with small-solid objects such as soils, small clay balls and food pellets (Deacon, 2006a). X11L-KO mice displaced significantly less food pellets from a tube (4–5 months old, $n = 14$ per group; WT, 80.6 ± 15.4 g; X11L-KO mice, 10.1 ± 1.9 g; weight of displaced pellets, $p <$ 0.001). These data indicate that X11L plays a crucial role in these species-typical behaviors, which likely reflect defensive behaviors, seeking safety, exploration and hoarding food seen in the wild (Dudek et al., 1983; Deacon, 2006a,b), and further suggest X11L-KO mice are less attracted to what are usually attractive stimuli.

Impaired species-typical behaviors and reduced social interaction in X11L-KO mice are rescued by the expression of X11L during development

To confirm the causal link between X11L and a specific behavior impaired in X11L-KO mice, we performed a rescue experiment using the Tet-regulated system, which is used for conditional expression in mice (Mayford et al., 1996). In normal WT mice, X11L is highly expressed in the forebrain (Nakajima et al., 2001). Therefore, *Camk2a-tTA* mice (Mayford et al., 1996; Gross et al., 2002) were used to express X11L selectively in the forebrain after birth. In the *TRE-hX11L:Camk2tTA* DTg mice (Fig. 4*A*), FLAG-hX11L and β-galactosidase are expected to be coexpressed in the same cells. Western blot analyses using antibodies against the C-terminal epitope of X11L and FLAG successfully detected the expression of FLAG-hX11L in adult DTg brains (Fig. 4*B*). LacZ staining revealed that β-galactosidase was strongly expressed in the forebrain region, as well as in some other regions, such as the substantia nigra, ventral tegmental area, and raphe (Fig. 4*C*). Western blot analysis revealed that X11L protein expression was completely depleted by administering 2 mg/ml DOX in the drinking water for 3 weeks, and then recovered to ~80% of the initial expression level within 1 week after the withdrawal of DOX (Fig. 4*D*).

To perform a rescue experiment using this system, we generated DTg mice under the X11L-KO background (DTg:X11L-KO mice). We first focused on the MBT. DTg:X11L-KO mice buried significantly more marbles than X11L-KO mice (4–5 months old, WT, 8.1 ± 1.2, $n = 21$; X11L-KO, 2.7 ± 0.7, $n = 27$; DTg:X11L-KO, 5.6 ± 1.0, $n = 29$; X11L-KO vs DTg:X11L-KO, $p < 0.05$) (Fig. 4*G*). The increased burying behavior in DTg:X11L-KO mice was not likely due to an increase in general activity as the horizontal activity of DTg:X11L-KO mice was slightly but significantly decreased compared with X11L-KO mice in the habituation session and indistinguishable from X11L-KO mice in the MBT session (habituation session, X11L-KO vs DTg:X11L-KO, $p < 0.05$; MBT session, X11L-KO vs DTg:X11L-KO; $p = 0.53$) (Fig. 4*J*).

To test whether X11L protein regulates marble burying behavior during information processing, the expression of FLAG-hX11L was acutely inhibited in DTg:X11L-KO mice in the adult stage by administering DOX (DTg:X11L-KO/DOXad). FLAG-hX11L proteins were not detected in DTg:X11L-KO/DOXad mice administered DOX in their drinking water (2 mg/ml) for 3 weeks (Fig. 4*E*). The DTg:X11L-KO/DOXad mice, however, still buried significantly more marbles compared with X11L-KO mice (4–5 months old, WT/DOXad, 9.4 ± 1.4, $n = 21$, X11L-KO/DOXad, 3.0 ± 0.7, $n = 27$; DTg:X11L-KO/DOXad, 6.8 ± 1.0, $n = 30$; X11L-KO/DOXad vs DTg:X11L-KO/DOXad, $p < 0.01$) (Fig. 4*H*). The recovery of burying behavior was not associated with an increase in general activity (Fig. 4*K*). These data suggest that the X11L protein is required during the developmental stages but not in adults, for normal marble burying behavior. The partial recovery may indicate incomplete expression and/or a cell type specificity of X11L in DTg mice.

To further confirm the role of X11L in developmental stages, we administered DOX (25 μg/ml) in the drinking water of the parents from the mating period through postnatal day 28. This concentration of DOX was sufficient to completely suppress the expression of FLAG-hX11L in DTg:X11L-KO mice (DTg:X11L-KO/DOXdev) (Fig. 4*F*). The expression of FLAG-hX11L did not recover after DOX withdrawal, even after 5 months, in DTg:X11L-KO/DOXdev mice, unlike the case of DOX administration in adults (Fig. 4*F*). The transgenic locus silenced during the developmental stage likely acquires irreversible modifications. The numbers of marbles buried by DTg:X11L-KO/DOXdev mice and

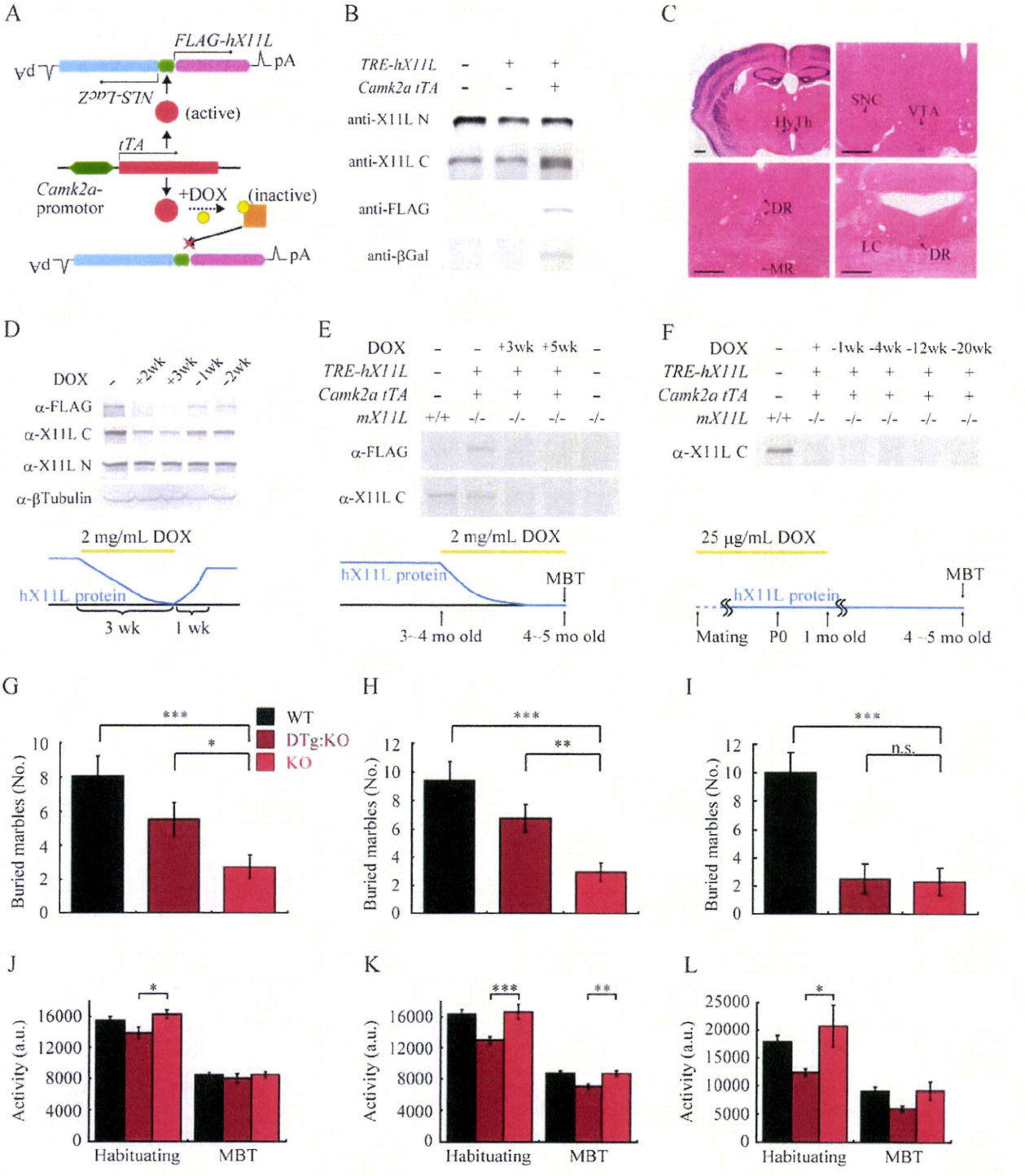

Figure 4. Impairment in marble burying behavior in X11L-KO mice was rescued by the expression of X11L during development, but not in adults. ***A***, The tTA protein is driven by *Camk2a* promoter. The active form of tTA binds to TRE and bidirectionally drives the expression of the *FLAG-hX11L* and *NLS-LacZ* genes. DOX inhibits the expression of both transgenes by binding to tTA and converting it into an inactive conformation. ***B***, Immunoblot of whole brain lysates obtained from transgenic and DTg mice. Anti-X11L N antibody only recognizes the N-terminal region of the mouse X11L protein. Anti-X11L C antibody recognizes the C-terminal region of both human and mouse X11L proteins. ***C***, Expression of the transgenes was detected by LacZ staining. Scale bars, 500 μm. HyTh, hypothalamus; SNC, substantia nigra pars compacta; VTA, ventral tegmental area; DR, dorsal raphe; MR, median raphe; LC, locus ceruleus. ***D***, Immunoblot of whole brain lysates obtained from DTg mice with administration and withdrawal of 2 mg/ml DOX in the drinking water. ***E***, Immunoblot of whole brain lysates obtained from DTg:X11L-KO and control mice. Complete depletion of X11L in DTg:X11L-KO mice by 2 mg/ml DOX administration was confirmed. ***F***, Immunoblot of whole brain lysate obtained from DTg:X11L-KO mice after withdrawal from 25 μg/ml DOX administration during the developmental period. ***D–F***, Experimental design and results are schematically represented at the bottom part of each panel. Blue lines indicate X11L protein level. ***G–L***, MBT and concurrent measurement of locomotor activity were performed using DTg:X11L-KO mice with the various DOX administration paradigms. ***G–I***, MBT. The number of marbles buried was counted for each genotype of experimental group: without DOX administration (***G***), with DOX administration during the adult period (***H***), and with DOX administration in the developmental period (***I***) with subsequent withdrawal of DOX administration. ***J–L***, Locomotor activity in MBT and habituating sessions for each experimental group without DOX administration (***J***), the same as ***G***, with DOX in the adult period (***K***), the same as (***H***), and with DOX in the developmental period (***L***), the same as ***I***. Data represent mean ± SE. $^{*}p < 0.05$, $^{**}p < 0.01$, $^{***}p < 0.001$ (WT mice, black column; DTg:X11L-KO mice, brown column; X11L-KO mice, red column).

X11L-KO/DOXdev mice were indistinguishable (4–5 months old, WT/DOXdev, 10.0 ± 1.4, $n = 16$; X11L-KO/DOXdev, 2.3 ± 1.0, $n = 16$; DTg:X11L-KO/DOXdev, 2.5 ± 1.1, $n = 15$; X11L-KO/DOXdev vs DTg:X11L-KO/DOXdev, $p = 0.77$) (Fig. 4*I*). These results further strengthened the notion that X11L has an important role during development.

Locomotor activity in DTg:X11L-KO mice treated with or without DOX was significantly lower than that in X11L-KO mice (Fig. 4*J–L*). Decreased locomotor activity in *Camk2a-tTA* mice was reported by another group (McKinney et al., 2008). This decreased locomotor activity might lead to an underestimation of the degree of the rescued phenotype in our experiments.

Next, we examined the impact of X11L expression on burrowing behavior. We also observed that DTg:X11L-KO mice displaced significantly more food pellets from a tube than X11L-KO mice (5–6 months old, DTg:X11L-KO, 144.7 ± 11.6 g, $n = 14$; X11L-KO, 30.5 ± 9.6 g, $n = 16$; weight of displaced pellets, $p < 0.001$).

Finally, we performed the resident-intruder test using DTg:X11L-KO and X11L-KO mice to confirm whether the expression of X11L can also restore the suppressed social interaction in X11L-KO mice as is the case in the MBT. Resident social interactions with intruder mice were significantly increased in DTg:X11L-KO mice compared with X11L-KO mice (4–5 months old, DTg:X11L-KO $n = 14$, X11L-KO $n = 16$; approach, $F_{(1,28)} = 5.86$, $p < 0.05$; following, $F_{(1,28)} = 4.32$, $p < 0.05$; aggression, $F_{(1,28)} = 0.22$, $p = 0.64$; social interaction, $F_{(1,28)} = 6.86$, $p < 0.05$; Figure 5*A–D*). These data indicate that X11L protein is required not only for normal burying/burrowing behavior but also for normal social behavior, and suggest that social behavior and species-typical behavior may share some common neuronal mechanisms associated with X11L protein.

Monoamine systems are disrupted in X11L-KO mice

Marble burying behavior is affected by anxiolytic drugs, particularly 5-HT agents. Drugs acting on the 5-HT system, such as 5-HT reuptake inhibitors, which increase 5-HT levels at release sites, and some 5-HT agonists, inhibit marble burying behavior without affecting locomotor activity (Njung'e and Handley, 1991b; Shinomiya et al., 2005; Nicolas et al., 2006; Bruins Slot et al., 2008). Some antipsychotics also inhibit marble burying behavior (Broekkamp et al., 1986; Nicolas et al., 2006; Bruins Slot et al., 2008). These reports suggest that monoaminergic activity underlie marble burying behavior. Therefore, we measured the amounts of monoamines and their metabolites in selected brain regions of X11L-KO mice.

Biopsies of the following seven regions were obtained from frozen brain sections: anterior cingulate cortex, striatum, hypothalamus (mainly containing the paraventricular nucleus), somatosensory cortex (mainly containing the barrel field), amygdala, hippocampus (mainly containing the CA3 region), and dorsal and median raphe (Fig. 6*A*). These areas were selected on the basis of high X11L expression, or their known involvement in the behaviors studied here. Although the levels of most monoamines and their metabolites in the X11L-KO mice brains were not significantly different from those in WT mice, 5-HT levels were significantly higher in the hypothalamus and somatosensory cortex (Table 1). Because monoamines are synthesized and broken down in sophisticated biochemical networks, we sought evidence of an altered flux through these networks by analyzing the correlations among monoamines and their metabolites. The correlational relationships in the striatum, hippocampus, and somatosensory cortex of X11L-KO mice were substantially different from those in WT mice, which were reflected in an asymmetrical pattern in the correlation maps (Fig. 6*B*). In contrast, these relationships were highly comparable in the raphe and amygdala (Fig. 6*B*). These results suggest that X11L has an active role in regulating the synthesis and/or breakdown of monoamine neurotransmitters.

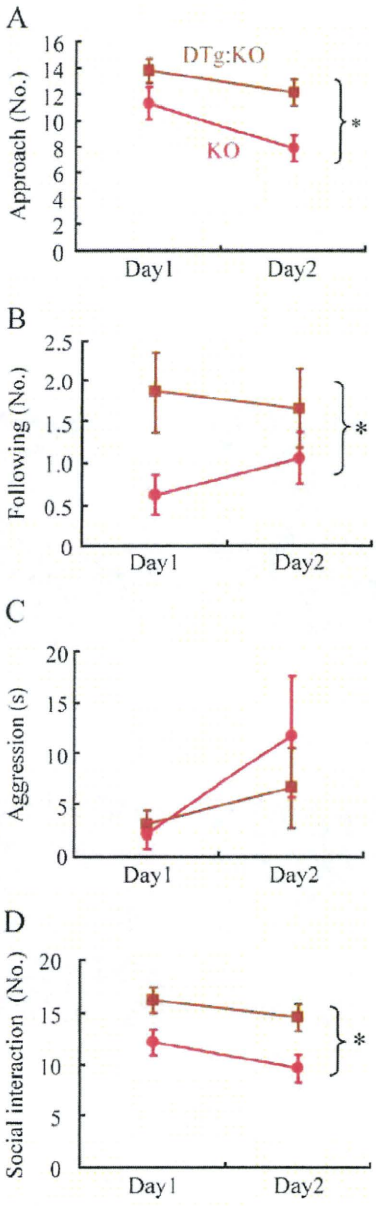

Figure 5. Reduced social interaction in X11L-KO mice was restored by the expression of the X11L protein. The resident-intruder test (DTg:X11L-KO mice, brown square; X11L-KO mice, red circle) was performed for 2 consecutive days using different intruder mice for each trial. ***A***, ***B***, The numbers of approaches (***A***) and following behaviors (***B***) of resident mice against intruder mice were significantly higher in DTg:X11L-KO mice. ***C***, Differences in the amount of time spent by resident mice exhibiting aggressive behavior was not statistically significant between genotypes. ***D***, The summed number of social interactions of resident mice toward intruder mice was significantly increased in DTg:X11L-KO mice compared with X11L-KO mice. Data represent mean ± SE. *$p < 0.05$.

To gain insight into the function of the serotonergic system in X11L-KO mice, we analyzed the hypothermic responses induced by the selective 5-HT1A receptor agonist 8-OH-DPAT, which reflects somatodendritic autoreceptor function in raphe neurons (Goodwin et al., 1985; Bill et al., 1991; Martin et al., 1992; Gross et

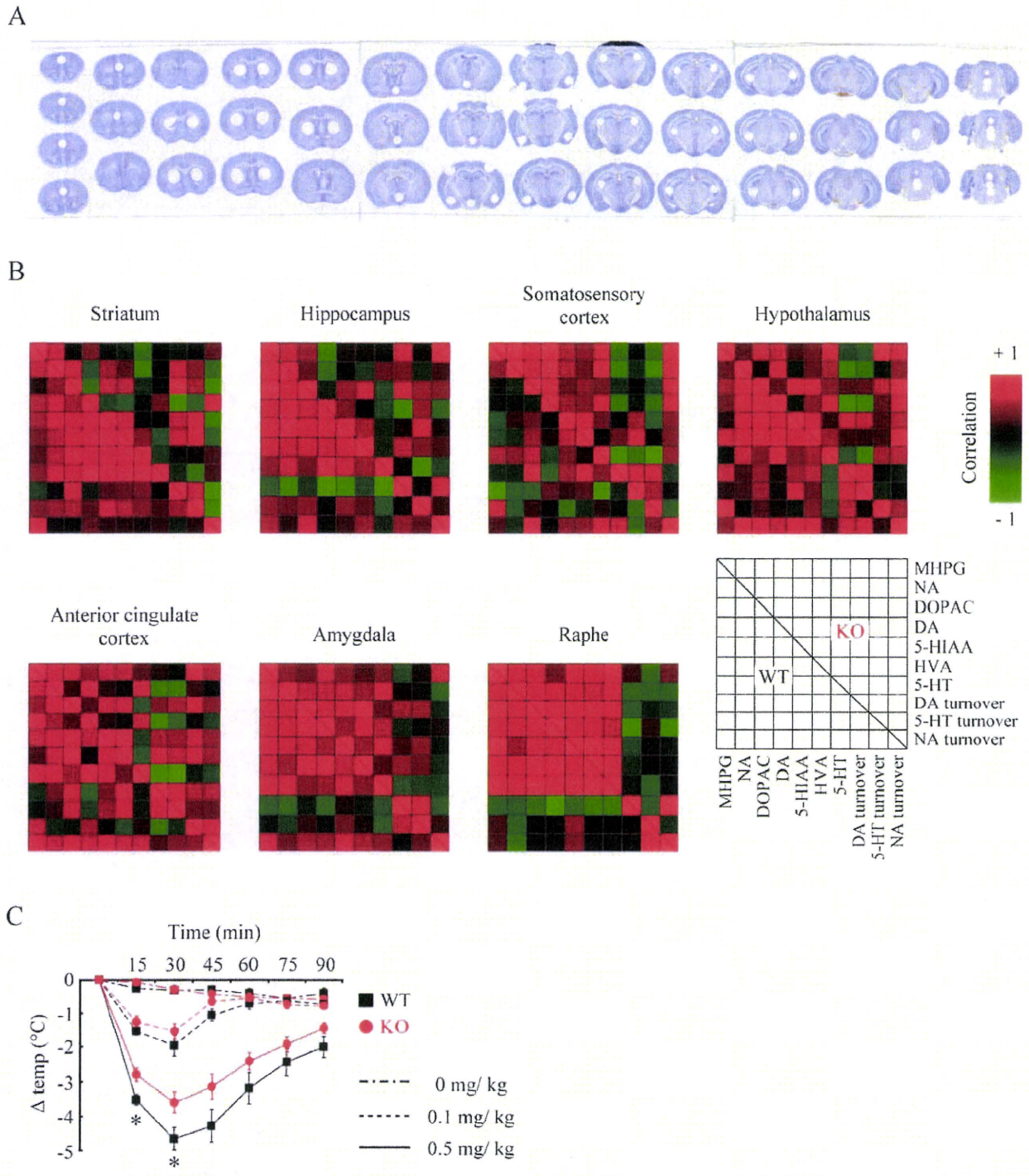

Figure 6. Balance of monoamine systems is disturbed in X11L-KO mice. ***A***, Representative photomicrographs of Nissl-stained brain sections showing locations of biopsies used for neurochemical analyses. ***B***, Correlation maps showing relationships between tissue contents of monoamines, metabolites, and calculated turnover values. Red indicates positive correlation. Green indicates negative correlation. ***C***, Time course and dose–response of 8-OH-DPAT-induced hypothermia in X11L-KO and WT mice. Data represent mean ± SE. *$p < 0.05$ (WT mice, black square; X11L-KO mice, red circle).

al., 2002). Stimulation of 5-HT1A autoreceptors attenuates 5-HT release and induces a hypothermic response. The body temperature of WT mice decreased after 8-OH-DPAT administration (Fig. 6*C*). This hypothermic response was significantly attenuated in X11L-KO mice 15 and 30 min after injection with 0.5 mg/kg 8-OH-DPAT (6–7 months old, WT and X11L-KO mice, $n = 8$ per group; at 15 and 30 min of 0.5 mg/kg dose, $p < 0.05$) (Fig. 6*C*), suggesting that 5-HT1A receptor function or its downstream signaling is attenuated in X11L-KO mice.

Discussion

The main finding of the present study is that X11L-KO mice show a selective deficit in motivated approach behavior, but not in motivated avoidance behavior. That is, X11L-KO mice showed

Table 1. The amount of monoamines and metabolites

Monoamines and metabolites	Genotypes	Anterior cingulate cortex	Striatum	Hypothalamus	Somatosensory cortex	Amygdala	Hippocampus	Raphe
5-HT	WT	1681 ± 144	2444 ± 165	4039 ± 170	917 ± 45	5403 ± 342	3566 ± 318	9779 ± 697
	KO	1491 ± 97	2709 ± 61	5021 ± 245**	1130 ± 78*	4819 ± 287	3464 ± 188	9069 ± 908
5-HIAA	WT	2300 ± 219	2500 ± 221	3939 ± 221	758 ± 23	3663 ± 235	4661 ± 381	11,438 ± 933
	KO	2148 ± 64	2620 ± 79	3964 ± 212	759 ± 54	3247 ± 209	4121 ± 211	10,006 ± 855
NA	WT	3420 ± 214	73 ± 11	13,750 ± 607	2275 ± 78	3539 ± 188	2713 ± 217	5644 ± 493
	KO	3129 ± 134	117 ± 27	15,455 ± 654	2562 ± 150	3142 ± 141	2584 ± 93	5988 ± 619
MHPG	WT	513 ± 40	29 ± 7	577 ± 67	169 ± 7	573 ± 39	277 ± 28	1042 ± 78
	KO	449 ± 37	42 ± 8	553 ± 51	168 ± 8	452 ± 22*	245 ± 18	990 ± 118
DA	WT	460 ± 37	10,9843 ± 8939	2431 ± 133	90 ± 4	5345 ± 451	219 ± 30	1156 ± 99
	KO	394 ± 21	12,0274 ± 3273	2605 ± 157	94 ± 9	4227 ± 401	189 ± 12	1138 ± 117
DOPAC	WT	502 ± 46	18,005 ± 2298	854 ± 49	146 ± 12	2040 ± 152	265 ± 29	639 ± 41
	KO	420 ± 22	21,580 ± 1520	826 ± 28	141 ± 11	1654 ± 186	237 ± 14	594 ± 52
HVA	WT	1113 ± 148	14,317 ± 1178	1293 ± 97	192 ± 17	2145 ± 169	289 ± 20	1300 ± 70
	KO	889 ± 63	14,513 ± 312	1215 ± 65	153 ± 17	1647 ± 198	273 ± 21	1233 ± 111
5-HT	WT	1.27 ± 0.07	0.94 ± 0.05	0.90 ± 0.05	0.77 ± 0.04	0.63 ± 0.03	1.22 ± 0.07	1.08 ± 0.04
Turnover	KO	1.37 ± 0.10	0.89 ± 0.03	0.74 ± 0.05*	0.63 ± 0.06	0.62 ± 0.03	1.12 ± 0.08	1.03 ± 0.04
NE	WT	0.14 ± 0.01	0.36 ± 0.06	0.04 ± 0.004	0.07 ± 0.003	0.15 ± 0.004	0.09 ± 0.003	0.17 ± 0.01
Turnover	KO	0.13 ± 0.01	0.36 ± 0.04	0.03 ± 0.003	0.06 ± 0.001*	0.13 ± 0.01	0.09 ± 0.005	0.16 ± 0.01
DA	WT	3.16 ± 0.53	0.26 ± 0.02	0.77 ± 0.03	3.30 ± 0.29	0.69 ± 0.02	2.36 ± 0.18	1.47 ± 0.05
Turnover	KO	2.92 ± 0.20	0.27 ± 0.02	0.69 ± 0.04	2.82 ± 0.20	0.69 ± 0.06	2.44 ± 0.24	1.44 ± 0.10

Data shown are mean ± SE (pg/mg protein).

significantly attenuated ethological responses to attractive stimuli and withdrew during approach-avoidance conflict, such as that encountered during competitive feeding conditions and social interaction. Additionally, attenuated marble-burying, burrowing and reduced social behavior in X11L-KO mice was rescued by expression of X11L protein during development. Together, these findings suggest that X11L is involved in the maturation of neuronal circuits regulating conflict resolution-related behaviors. We propose that X11L-KO mice provide a novel model for analyzing emotional behavior, which differs from the existing models of generalized anxiety-like and depression-like behaviors (Finn et al., 2003; Cryan and Mombereau, 2004; Crawley, 2007).

X11L-KO mice lost more body weight than WT mice, specifically under a competitive feeding regimen with WT mice. This was unlikely due to physical defects or changes in general activity, but is likely related to the suppression of a social interaction-induced behavioral response. The results from the resident-intruder test support this notion. That is, X11L-KO mice exhibited reduced exploratory behavior toward intruder mice. The social behavior of one mouse toward another mouse probably reflects the net result of conflicts from coexisting incentives, including those that might induce approach (e.g., investigation of intruder mice and approach to housemates that have a food pellet) and those that might induce avoidance (e.g., threat from novel intruders, avoiding competition with housemates, and generalized anxiety). Anxiety-like behaviors, which are often expressed as avoidance, are thought to be closely associated with decreased social interaction (File, 1992; Sankoorikal et al., 2006; Crawley, 2007; Moy et al., 2007). Interestingly, X11L-KO mice did not show anxiety-like behavior in standard behavioral tests, such as the elevated plus maze, light and dark transition, and open field tests. Thus, low levels of social interaction in X11L-KO mice appear to be independent of "traditional" anxiety-like behaviors that are expressed as avoidance of aversive stimuli.

X11L-KO mice showed prominent defective ethological stimuli-responses, such as reduced burying, digging and burrowing behaviors, whereas they showed no phenotypes in many of the most common behavioral tests (e.g., locomotor activity, circadian rhythm, open field, elevated plus maze, light and dark transition, tail suspension, prepulse inhibition and some learning/memory tests) commonly applied in the study of behavioral genetics. These data highlight the importance of testing species-typical behaviors to better understand brain functions. So-called ethological tests likely have strong potential to extract brain function and mechanisms. Burrowing behavior is highly sensitive to dysfunctions of the hippocampus induced by cytotoxic lesion, scrapie infection and in AD model mice (Deacon et al., 2001, 2002, 2008). Marble burying behavior is correlated very well with activity in the serotonin system and is proposed to have predictive validity as a model of obsessive-compulsive disorder (OCD)-like behavior as drugs used to treat OCD inhibit marble burying behavior (Njung'e and Handley, 1991b; Shinomiya et al., 2005; Nicolas et al., 2006; Bruins Slot et al., 2008; Kobayashi et al., 2008). Thus, species-typical ethological responses may provide the most sensitive parameters to estimate the therapeutic effect using animal models.

Transgene rescue experiments using the *Camk2a-tTA* mouse line suggested that X11L is involved in the development of neuronal circuits regulating emotional and conflict-related behaviors. We found that monoamine concentrations in forebrain regions of X11L-KO mice were imbalanced. Monoamine signaling is critically involved in developing neuronal circuits that modulate emotion in adults (Reif and Lesch, 2003). The development of 5-HT function in the postnatal period determines adult emotional behavior (Andersen et al., 2002; Gross et al., 2002; Ansorge et al., 2004, 2008; Lo Iacono and Gross, 2008). Catecholamine levels during early life also influence adult emotional behavior (Estelles et al., 2007; Gray et al., 2007). Maturation and/or refinement of forebrain circuits during postnatal weeks 2 through 5 via somatodendritic 5HT1A receptor interactions is considered critical for programming anxiety-related behaviors (Gross et al., 2002; Lo Iacono and Gross, 2008). X11L expression begins during development, is strongly localized to the somatodendritic compartment of forebrain region (Nakajima et al., 2001; Ho et al., 2003), and binds many molecules involved in regulating neuronal activity. Therefore, X11L may function as a neuronal media-

tor in the development of emotional circuits via molecules relating to monoaminergic systems.

Alternatively, or additionally, the behavioral deficits observed in X11L-KO mice in adulthood may reflect ongoing neurochemical perturbations. In the present study, the statistically strongest neurochemical difference was increased 5-HT content in the hypothalamus. Previous studies show that decreased hypothalamic 5-HT levels are associated with increased aggression in rats [Vergnes et al., (1988); see Popova (2006) for discussion of the role of 5-HT in aggression]. By the same token, the subordinate behavior of X11L-KO mice reported here may relate to increased 5-HT levels and/or altered 5-HT metabolism. It should be noted, however, that monoamine turnover rates were marginally lower in X11L-KO mice in some regions studied, in addition to monoamine-metabolite imbalances being evident. Thus, the possibility that other neurochemical changes underlie the behavioral deficits observed here cannot be ruled out. There is undoubtedly a close relationship between activity in monoaminergic systems, as exemplified by studies of 5-HT1A and 5-HT1B receptor KO mice, which show increases in both 5-HT and dopamine turnover (Ase et al., 2000). Indeed, all three monoaminergic systems are targeted in the treatment of anxiety-related disorders and social phobias in the clinical setting, and so much further research is necessary to elucidate the detailed interactions between these systems that bring about the sophisticated behaviors studied here.

How X11L affects monoaminergic systems remains to be determined. 8-OH-DPAT (5-HT1A receptor specific antagonist)-induced hypothermia was attenuated in the X11L-KO mice. The 5-HT1A receptor is a G_i-type G-protein coupled receptor. Its activation opens G-protein-coupled inwardly rectifying K^+ channels (GIRKs) by binding liberated $G_\beta\gamma$ proteins from 5-HT1A receptor, resulting in cell hyperpolarization and inhibition of 5-HT release (Andrade and Nicoll, 1987; Williams et al., 1988; Lüscher et al., 1997). Functional coupling of 5-HT1A receptors to GIRKs does not occur until postnatal day 14 (Béïque et al., 2004). GIRKs are also downstream regulators of several other G-protein coupled receptors such as dopaminergic (D2), adrenergic (α2), and muscarinic (M2) autoreceptors, and they act to regulate cellular excitability and coupling (North, 1989; Hille, 1992; Yamada et al., 1998). GIRKs containing the GIRK2 subunit are control hubs for the hypothermic response induced by various G-protein coupled receptor agonists (Costa et al., 2005). The GIRK2 subunit is widely distributed throughout the brain and strongly localized to the somatodendritic compartment (Murer et al., 1997; Schein et al., 1998; Inanobe et al., 1999; Saenz del Burgo et al., 2008). Additionally, GIRK3 and GIRK2c, which is a splice variant of GIRK2, subunits have a PDZ-binding motif (-ESKV) at their C-terminal and their trafficking is regulated by PDZ-containing adaptor proteins (Inanobe et al., 1999; Ma et al., 2002; Lunn et al., 2007). In contrast, X11L regulates the intracellular localization of its binding protein and also has coat protein properties (Hill et al., 2003; Sano et al., 2006a). Therefore, it is possible that X11L regulates the intracellular localization of GIRK2, and the functional attenuation of GIRKs, by ultimately altering neuronal excitability, may disturb monoamine balance and reduce the hypothermic response in X11L-KO mice. Indeed, we have observed specific binding between X11L and GIRK2c by coimmunoprecipitation analyses using a cell culture system (YS, HS, and SI, unpublished data).

Other mechanisms may underlie the role of X11L in neurochemical activity and behavior. X11L regulates APP metabolism (Sano et al., 2006a) and interacts with many other types of neuronal/synaptic machinery (Okamoto and Südhof, 1997; Tomita et al., 1999; Biederer and Südhof, 2000; Gotthardt et al., 2000; Lau et al., 2000; Kitano et al., 2002; Araki et al., 2003; Hill et al., 2003; Kimura et al., 2004). The unique behavioral abnormalities in X11L-KO mice may be due to the combined dysfunction of interacting molecules and the compensatory effect of X11, which has binding partners and cellular functions similar to those of X11L (Ho et al., 2006; Miller et al., 2006; Rogelj et al., 2006; Sano et al., 2006a). Interestingly, compared with WT mice, X11-KO mice exhibit a vigorous and rapid escape response when the sides and body of the animal are stroked (Mori et al., 2002). Comparative studies using these mice and mice with conditional double mutations in limited subsets of neurons might help to better understand the mechanisms that underlie emotional control.

Finally, the X11L gene, namely *APBA2*, is located at the 15q11-q12 locus. The close association between abnormalities in the 15q11-q13 region and autism is frequently reported (Cook et al., 1997, 1998; Gillberg, 1998; Schroer et al., 1998; Shao et al., 2002; Muhle et al., 2004). Autism is a neurodevelopmental disorder characterized by impaired social interaction and communication. It is possible that X11L dysfunction during the developmental stage relates to the pathogenesis of developmental disorders with mental retardation such as autism, and X11L may have an important role in the development of emotionality and sociability in humans.

References

Andersen SL, Dumont NL, Teicher MH (2002) Differences in behavior and monoamine laterality following neonatal clomipramine treatment. Dev Psychobiol 41:50–57.

Andrade R, Nicoll RA (1987) Pharmacologically distinct actions of serotonin on single pyramidal neurones of the rat hippocampus recorded in vitro. J Physiol 394:99–124.

Ansorge MS, Zhou M, Lira A, Hen R, Gingrich JA (2004) Early-life blockade of the 5-HT transporter alters emotional behavior in adult mice. Science 306:879–881.

Ansorge MS, Morelli E, Gingrich JA (2008) Inhibition of serotonin but not norepinephrine transport during development produces delayed, persistent perturbations of emotional behaviors in mice. J Neurosci 28:199–207.

Araki Y, Tomita S, Yamaguchi H, Miyagi N, Sumioka A, Kirino Y, Suzuki T (2003) Novel cadherin-related membrane proteins, Alcadeins, enhance the X11-like protein-mediated stabilization of amyloid beta-protein precursor metabolism. J Biol Chem 278:49448–49458.

Ase AR, Reader TA, Hen R, Riad M, Descarries L (2000) Altered serotonin and dopamine metabolism in the CNS of serotonin 5-HT(1A) or 5-HT(1B) receptor knockout mice. J Neurochem 75:2415–2426.

Béïque JC, Campbell B, Perring P, Hamblin MW, Walker P, Mladenovic L, Andrade R (2004) Serotonergic regulation of membrane potential in developing rat prefrontal cortex: coordinated expression of 5-hydroxytryptamine (5-HT)1A, 5-HT2A, and 5-HT7 receptors. J Neurosci 24:4807–4817.

Biederer T, Südhof TC (2000) Mints as adaptors. Direct binding to neurexins and recruitment of munc18. J Biol Chem 275:39803–39806.

Bill DJ, Knight M, Forster EA, Fletcher A (1991) Direct evidence for an important species difference in the mechanism of 8-OH-DPAT-induced hypothermia. Br J Pharmacol 103:1857–1864.

Broekkamp CL, Rijk HW, Joly-Gelouin D, Lloyd KL (1986) Major tranquillizers can be distinguished from minor tranquillizers on the basis of effects on marble burying and swim-induced grooming in mice. Eur J Pharmacol 126:223–229.

Bruins Slot LA, Bardin L, Auclair AL, Depoortere R, Newman-Tancredi A (2008) Effects of antipsychotics and reference monoaminergic ligands on marble burying behavior in mice. Behav Pharmacol 19:145–152.

Chapman PF, White GL, Jones MW, Cooper-Blacketer D, Marshall VJ, Irizarry M, Younkin L, Good MA, Bliss TV, Hyman BT, Younkin SG, Hsiao KK (1999) Impaired synaptic plasticity and learning in aged amyloid precursor protein transgenic mice. Nat Neurosci 2:271–276.

Chen G, Chen KS, Knox J, Inglis J, Bernard A, Martin SJ, Justice A, McCon-